$B_u \to \psi M$ decays and S-D wave mixing effects*

Yueling Yang(杨悦玲) Yupei Guo(郭育培) Junfeng Sun(孙俊峰)[1)] Na Wang(王娜)
Qin Chang(常钦) Gongru Lu(鲁公儒)

Institute of Particle and Nuclear Physics, Henan Normal University, Xinxiang 453007, China

Abstract: The $B_u \to \psi M$ decays are studied with the perturbative QCD approach, where the psion $\psi = \psi(2S)$, $\psi(3770)$, $\psi(4040)$ and $\psi(4160)$, and the light meson $M = \pi$, K, ρ and K^*. The factorizable and non-factorizable contributions, and the S-D wave mixing effects on the psions, are considered in the calculation. With appropriate inputs, the branching ratios for the $B_u \to \psi K$ decays are generally coincident with the experimental data within errors. However, due to the large theoretical and experimental errors, it is impossible for the moment to give a severe constraint on the S-D wave mixing angles.

Keywords: B meson, weak decay, psion, perturbative QCD

PACS: 12.15.Ji, 12.39.St, 13.25.Hw **DOI:** 10.1088/1674-1137/42/11/113102

1 Introduction

The exclusive B meson decays into one psion (ψ) and one light meson (M) are of great interest, and have attracted much attention over past years. In this paper, unless otherwise specified, the symbol ψ denotes the high excited charmonium states with the quantum numbers[2)] $I^GJ^{PC} = 0^-1^{--}$, including $\psi(2S)$[3)], $\psi(3770)$[4)], $\psi(4040)$[4)], and $\psi(4160)$[4)] [1]; and the symbol M refers to the members of the ground $SU(3)$ pseudoscalar P and vector V meson nonet; $P = \pi$ and K, and $V = \rho$ and K^*. From the theoretical point of view, the $B \to \psi M$ decays are predominantly induced by the process $b \to c + W^{*-} \to c + \bar{c}q$ ($q = d$ or s) with the spectator quark ansatz. The c quark originating from the b quark decay must unite with the $\bar{c}$ quark arising from the virtual W^{*-} decay to form the flavor-singlet psion. In addition, the color charges of the c and $\bar{c}$ quarks from two different sources must match with each other to be colorless. Hence, the $B \to \psi M$ decays induced by the internal W-emission interactions are color suppressed (class-II), in comparison with the non-leptonic B weak decays induced by the external W-emission interactions (class-I).

Phenomenologically, the non-leptonic B meson weak decays have been studied carefully within the framework of the factorization hypothesis and the low-energy effective Hamiltonian [4]. The naive factorization (NF) assumption [5–7] is usually employed in evaluating the non-leptonic B meson decays, where the decay amplitudes in terms of hadronic matrix elements (HMEs) of the four-quark operators can be expressed as the product of two HMEs of the diquark currents, based on Bjorken's color transparency argument [8]. The diquark HME can be further parameterized by the decay constants or the hadron transition form factors. The NF hypothesis was verified experimentally to be successful for the class-I non-leptonic B decays, but poor for the class-II ones. It is commonly believed that the characteristic space configuration of psions is compact, with a radius of $r \sim 1/m_c$. The transverse separation between the two valence charm quarks should be very small. The massive psions from the B meson decay can be regarded as color singlet states and factorized from the other system, although the velocity of the psion might be not very large. The class-II $B \to J/\psi(1S)M$ decays have been stud-

Received 21 June 2018, Published online 13 October 2018

∗ Supported by the National Natural Science Foundation of China (11705047, U1632109, 11547014, 11475055) and Open Research Program of Large Research Infrastructures (2017), Chinese Academy of Sciences

1) E-mail: sunjunfeng@htu.edu.cn

2) The symbols I, J, G, P, and C refer to the isospin, angular momentum, G-parity, P-parity, and C-parity of one particle, respectively.

3) The symbols nL in parentheses are the radial quantum number n and the orbital angular momentum L, with $n = 1, 2, \cdots$, and $L = S, P, D, \cdots$. The $\psi(2S)$ particle is thought to be a $2S$-wave dominated charmonium state, possibly with some D-wave components.

4) The numbers in parentheses indicate the approximate masses of the particles in the unit of MeV. The dominant components of the particles $\psi(3770)$, $\psi(4040)$ and $\psi(4160)$ are usually considered as the 1^3D_1, 3^3S_1 and 2^3D_1 states, respectively [1–3]. Here, the spectroscopic notation $n^{2s+1}L_J$ is used, where s is the total spin of the quark-antiquark pair, and J is the total angular momentum.

ied based on the factorization assumption, for example in Refs. [9–18], where besides the factorizable contributions, the non-factorizable contributions beyond the NF approximation are also taken into account to accommodate the discrepancies between the experimental data and the theoretical estimations. The $B \to \psi M$ decays provide a good place to check the factorization postulation and differentiate various theoretical treatments, such as the QCD factorization (QCDF) approach [19–37] based on the collinear approximation, and the perturbative QCD (pQCD) approach [38–47] based on the collinear plus k_T factorization supposition.

It is well known that according to the quark model assignments, spin-triplet charmonium states with different orbital angular momentum L can have the same quantum numbers J^{PC}. The conservation of parity and angular momentum implies that the values of L for the mixed states can differ by two units at most. The psions near and above the open-charm threshold can be admixtures of the S- and D-wave $c\bar{c}$ states [48–60]. The wave functions for the S-wave dominant state can receive the D-wave component and vice versa. Additionally, studies of the charmonium spectrum [61–64] show that the mass of the n^3S_1 state is close to the mass of the $(n{-}1)^3D_1$ state. To the first-order approximation, the so-called S-D wave mixing for psions refers mainly to the mixing between the n^3S_1 and $(n{-}1)^3D_1$ charmonium states rather than the other states, and this has been used in previous studies [48–60]. This S-D wave mixing phenomenon might have certain effects on the production of psions in the $B \to \psi M$ decays.

In this paper, we will investigate the $B_u \to \psi M$ decays with the pQCD approach. Firstly, the electrically charged final meson M should be easily identified by many specific detectors at the existing and future high energy colliders because of its track curve being saturated with the magnetic field. Secondly, the practicability of the pQCD approach can be checked with the class-II B decays into final states containing the excited psions. Thirdly, the effects of the S-D wave mixing among psions can be examined with the $B_u \to \psi M$ decays, without the disturbances from the mixing between the neutral B mesons and without the pollution from the weak annihilation contributions.

This paper is organized as follows. The theoretical framework and the amplitudes for the $B_u \to \psi M$ decays are elaborated in Section **2**. The numerical results and discussion are presented in Section **3**. Finally, we give a short summary in Section **4**.

2 Theoretical framework

2.1 The effective Hamiltonian

The $B_u \to \psi M$ decays are actually induced by the weak interaction cascade processes $b \to c + W^{*-} \to c + \bar{c}q$ at the quark level within the standard model. Hence, some relevant energy scales are introduced theoretically, such as the infrared confinement scale $\Lambda_{\rm QCD}$ of the strong interactions, the mass m_b for the decaying bottom quark, and the mass m_W for the virtual gauge boson W^*, with the clear size relation $\Lambda_{\rm QCD} \ll m_b \ll m_W$. The effective theory is usually used in practice to deal with realistic multi-scale problems. With the operator product expansion and the renormalization group (RG) method, the effective Hamiltonian in charge of the $B_u \to \psi M$ decays can be written as [4],

$$\begin{aligned}\mathcal{H}_{\rm eff} = \frac{G_{\rm F}}{\sqrt{2}}\sum_{q=d,s}\Bigg\{V_{cb}V_{cq}^*\sum_{i=1}^{2}C_i(\mu)Q_i(\mu) \\ -V_{tb}V_{tq}^*\sum_{j=3}^{10}C_j(\mu)Q_j(\mu)\Bigg\}+{\rm h.c.},\end{aligned} \tag{1}$$

where the Fermi coupling constant $G_{\rm F} \simeq 1.166{\times}10^{-5}{\rm GeV}^{-2}$ [1]. $V_{pb}V_{pq}^*$ is the product of the Cabibbo-Kobayashi-Maskawa (CKM) matrix elements, satisfying the unitarity relation $V_{ub}V_{uq}^* + V_{cb}V_{cq}^* + V_{tb}V_{tq}^* = 0$. With the Wolfenstein parametrization, the CKM factors can be expanded as the power series of the parameter $\lambda \approx 0.2$ [1]. Up to $\mathcal{O}(\lambda^7)$, these CKM factors can be written as follows:

$$V_{cb}V_{cd}^* = -A\lambda^3{+}\mathcal{O}(\lambda^7), \tag{2}$$

$$V_{tb}V_{td}^* = A\lambda^3(1{-}\rho{+}{\rm i}\eta){+}\frac{1}{2}A\lambda^5(\rho{-}{\rm i}\eta){+}\mathcal{O}(\lambda^7), \tag{3}$$

$$V_{cb}V_{cs}^* = A\lambda^2{-}\frac{1}{2}A\lambda^4{-}\frac{1}{8}A\lambda^6(1{+}4A^2){+}\mathcal{O}(\lambda^7), \tag{4}$$

$$V_{tb}V_{ts}^* = -V_{cb}V_{cs}^*{-}A\lambda^4(\rho{-}{\rm i}\eta){+}\mathcal{O}(\lambda^7). \tag{5}$$

From the expression for $V_{pb}V_{pq}^*$ above, it is clearly seen that the weak phases for the $B_u \to \psi M$ decays are small, and thus result in a small direct CP violation.

The renormalization scale μ divides the physical contributions into the short- and long-distance parts. The physical contributions from the scale larger than μ are summarized in the Wilson coefficients C_i. The Wilson coefficients, $\vec{C}_i = \{C_1,C_2,\cdots,C_{10}\}$, are calculable at the scale $\mu_W \sim \mathcal{O}(m_W)$ with perturbation theory, and then evolved to the characteristic scale $\mu_b \sim \mathcal{O}(m_b)$ for the b quark decay with the RG equation [4],

$$\vec{C}_i(\mu_b){=}U(\mu_b,\mu_W)\vec{C}_i(\mu_W), \tag{6}$$

where $U(\mu_b,\mu_W)$ is the RG evolution matrix. The Wilson coefficients are independent of any process and have the same role as the universal gauge couplings. The expressions of the Wilson coefficients $\vec{C}_i(m_W)$ and $U(\mu_b,\mu_W)$, including the next-to-leading order (NLO) corrections, can be found in Ref. [4]. The physical contributions from the scale less than μ are incorporated into the HME,

$\langle\psi M|Q_i|B_u\rangle$, where the local four-quark operators Q_i are sandwiched between the initial and final hadron states. The operators are expressed as follows:

$$Q_1 = \bar{c}_\alpha\gamma_\mu(1-\gamma_5)b_\alpha\ \bar{q}_\beta\gamma^\mu(1-\gamma_5)c_\beta, \tag{7}$$

$$Q_2 = \bar{c}_\alpha\gamma_\mu(1-\gamma_5)b_\beta\ \bar{q}_\beta\gamma^\mu(1-\gamma_5)c_\alpha, \tag{8}$$

$$Q_3 = \sum_{q'}\bar{q}_\alpha\gamma_\mu(1-\gamma_5)b_\alpha\ \bar{q}'_\beta\gamma^\mu(1-\gamma_5)q'_\beta, \tag{9}$$

$$Q_4 = \sum_{q'}\bar{q}_\alpha\gamma_\mu(1-\gamma_5)b_\beta\ \bar{q}'_\beta\gamma^\mu(1-\gamma_5)q'_\alpha, \tag{10}$$

$$Q_5 = \sum_{q'}\bar{q}_\alpha\gamma_\mu(1-\gamma_5)b_\alpha\ \bar{q}'_\beta\gamma^\mu(1+\gamma_5)q'_\beta, \tag{11}$$

$$Q_6 = \sum_{q'}\bar{q}_\alpha\gamma_\mu(1-\gamma_5)b_\beta\ \bar{q}'_\beta\gamma^\mu(1+\gamma_5)q'_\alpha, \tag{12}$$

$$Q_7 = \sum_{q'}\frac{3}{2}e_{q'}\bar{q}_\alpha\gamma_\mu(1-\gamma_5)b_\alpha\ \bar{q}'_\beta\gamma^\mu(1+\gamma_5)q'_\beta, \tag{13}$$

$$Q_8 = \sum_{q'}\frac{3}{2}e_{q'}\bar{q}_\alpha\gamma_\mu(1-\gamma_5)b_\beta\ \bar{q}'_\beta\gamma^\mu(1+\gamma_5)q'_\alpha, \tag{14}$$

$$Q_9 = \sum_{q'}\frac{3}{2}e_{q'}\bar{q}_\alpha\gamma_\mu(1-\gamma_5)b_\alpha\ \bar{q}'_\beta\gamma^\mu(1-\gamma_5)q'_\beta, \tag{15}$$

$$Q_{10} = \sum_{q'}\frac{3}{2}e_{q'}\bar{q}_\alpha\gamma_\mu(1-\gamma_5)b_\beta\ \bar{q}'_\beta\gamma^\mu(1-\gamma_5)q'_\alpha, \tag{16}$$

where $Q_{1,2}$ are the tree operators originating from the W-boson emission; $Q_{3,\cdots,6}$ and $Q_{7,\cdots,10}$ are the QCD and electroweak penguin operators, respectively; $(q_1q_2)_{V\pm A} = q_1\gamma_\mu(1\pm\gamma_5)q_2$; α and β are color indices, i.e., the QCD corrections are considered; q' denotes all the active quarks at the scale of $\mathcal{O}(m_b)$, i.e., $q' = u$, d, c, s, b; and $e_{q'}$ is the fractional electric charge of the quark q' in the unit of $|e|$. To obtain the decay amplitudes, the proper calculation of the HME $\langle\psi M|Q_i|B_u\rangle$ is the focus of the current research.

2.2 Hadronic matrix elements

The participation of the strong interaction greatly complicates the theoretical calculation of HMEs for the non-leptonic B weak decays in a reliable way, because of the entanglement between the perturbative and non-perturbative contributions. To evaluate the non-factorizable contributions to HMEs beyond the NF approximation [5–7], many QCD-inspired phenomenological approaches, such as the QCDF [19–37] and pQCD [38–47] approaches, have been developed recently, based on the framework proposed by Lepage and Brodsky [65]. The short- and long-distance contributions are effectively coordinated, and the HMEs are written as the convolution of the universal wave functions (WFs) reflecting the non-perturbative contributions with the process-dependent hard scattering amplitudes containing perturbative contributions. With the pQCD approach, it is supposed that the final M meson should be energetic in the rest frame of the initial B_u meson. The soft spectator quark of the B_u meson, carrying momentum of $\mathcal{O}(\Lambda_{\rm QCQ})$, should be kicked by one hard gluon so that the spectator quark can move as fast as the light quark from the bottom quark weak decay and then be incorporated into the color-singlet M meson. That means the spectator quark should interact with other quarks via one hard gluon exchange. In the practical calculation, in order to circumvent the endpoint singularities appearing in the collinear approximation [22–25], the pQCD approach suggests [38–40] retaining the transverse momentum of the valence quarks and simultaneously introducing the Sudakov factors for all participant meson WFs to further depress the non-perturbative contributions. Finally, the pQCD decay amplitudes are divided into three parts [39–47]: the hard contributions enclosed by the Wilson coefficients C_i, the bottom quark scattering amplitudes $\mathcal{H}_i$, and the non-perturbative contributions absorbed into the mesonic WFs Φ_i. The general form is a multidimensional integral,

$$\mathcal{A}_i \propto \int\prod_j dx_j db_j C_i(t_i)\mathcal{H}_i(t_i,x_j,b_j)\Phi_j(x_j,b_j)\mathrm{e}^{-S_j}, \tag{17}$$

where x_j is the longitudinal momentum fraction of the valence quarks; b_j is the conjugate variable of the transverse momentum k_{jT}; t_i is a typical scale; and e^{-S_j} is the Sudakov factor. In the numerical evaluations, besides the effective suppression of the long-distance contributions from the Sudakov factor, the scale t_i is usually chosen to be the maximum virtuality of all the internal particles, as shown in Eq. (B37), to further guarantee that the perturbative calculation of scattering amplitudes is practicable.

2.3 Kinematic variables

In the heavy quark limit, the light quark from the bottom quark decay is assumed to fly quickly away from the interaction point at near the speed of light. The light-cone dynamics can be used to describe the relativistic system. The relations between the four-dimensional space-time coordinates $(x^0, x^1, x^2, x^3) = (t, x, y, z)$ and the light-cone coordinates $(x^+, x^-, x_\perp)$ are defined as $x^\pm = (x^0\pm x^3)/\sqrt{2}$ and $x_\perp = (x^1, x^2)$. The planes of $x^\pm = 0$ are called the light-cone. The scalar product of any two vectors is given by $a\cdot b = a_\mu b^\mu = a^+b^- + a^-b^+ - a_\perp\cdot b_\perp$. In the rest frame of the B_u meson, the final ψ and M mesons move in the opposite direction. The light-cone kinematic variables are defined as follows.

$$p_B = p_1 = \frac{m_1}{\sqrt{2}}(1,1,0), \tag{18}$$

$$p_\psi = p_2 = (p_2^+, p_2^-, 0), \tag{19}$$

$$p_M = p_3 = (p_3^-, p_3^+, 0), \tag{20}$$

$$k_i = x_i p_i + (0,0,k_{iT}), \tag{21}$$

$$p_i^{\pm} = (E_i \pm p_{\rm cm})/\sqrt{2}, \tag{22}$$

$$t = 2p_1\cdot p_2 = 2m_1 E_2, \tag{23}$$

$$u = 2p_1\cdot p_3 = 2m_1 E_3, \tag{24}$$

$$s = 2p_2\cdot p_3, \tag{25}$$

$$st + su - tu = 4m_1^2 p_{\rm cm}^2, \tag{26}$$

where the subscript i = 1, 2, 3 on variables (including the mass m_i, momentum p_i and energy E_i) correspond to the B_u, ψ and M mesons, respectively. The parameters k_i, x_i, k_{iT} are the momentum, the longitudinal momentum fraction, and the transverse momentum of the valence antiquark, respectively. $p_{\rm cm}$ is the center-of-mass momentum of the final states.

2.4 Wave functions

The wave functions and/or distribution amplitudes (DAs) are the essential ingredient in the master pQCD formula of Eq. (17). Although non-perturbative, the WFs and DAs are generally considered to be universal for any process. The WFs and DAs determined by non-perturbative methods or extracted from data can be employed here to make predictions. Following the notations in Refs. [66–74], the WFs in question are defined as follows:

$$\langle 0|\bar{u}_i(z) b_j(0)|B_u^-(p)\rangle = \frac{if_B}{4}\int {\rm d}^4k {\rm e}^{-ik\cdot z}\left\{\left[\not{p}\Phi_B^a(k) + m_B\Phi_B^p(k)\right]\gamma_5\right\}_{ji}, \tag{27}$$

$$\langle \psi(p,\epsilon^{\parallel})|\bar{c}_i(z)c_j(0)|0\rangle = \frac{f_\psi}{4}\int {\rm d}^4k {\rm e}^{+ik\cdot z}\left\{\not{\epsilon}^{\parallel}\left[m_\psi\Phi_\psi^v(k) + \not{p}\Phi_\psi^t(k)\right]\right\}_{ji}, \tag{28}$$

$$\langle \psi(p,\epsilon^{\perp})|\bar{c}_i(z)c_j(0)|0\rangle = \frac{f_\psi}{4}\int {\rm d}^4k {\rm e}^{+ik\cdot z}\left\{\not{\epsilon}^{\perp}\left[m_\psi\Phi_\psi^V(k) + \not{p}\Phi_\psi^T(k)\right]\right\}_{ji}, \tag{29}$$

$$\langle P(p)|\bar{q}_i(z)q_j'(0)|0\rangle = \frac{1}{4}\int {\rm d}^4k {\rm e}^{+ik\cdot z}\left\{\gamma_5\left[\not{p}\Phi_P^a(k) + \mu_P\Phi_P^p(k) + \mu_P(\not{n}_+\not{n}_- - 1)\Phi_P^t(k)\right]\right\}_{ji}, \tag{30}$$

$$\langle V(p,\epsilon^{\parallel})|\bar{q}_i(z)q_j'(0)|0\rangle = \frac{1}{4}\int {\rm d}^4k {\rm e}^{+ik\cdot z}\left\{\not{\epsilon}^{\parallel} m_V\Phi_V^v(k) + \not{\epsilon}^{\parallel}\not{p}\Phi_V^t(k) - m_V\Phi_V^s(k)\right\}_{ji}, \tag{31}$$

$$\langle V(p,\epsilon^{\perp})|\bar{q}_i(z)q_j'(0)|0\rangle = \frac{1}{4}\int {\rm d}^4k {\rm e}^{+ik\cdot z}\left\{\not{\epsilon}^{\perp} m_V\Phi_V^V(k) + \not{\epsilon}^{\perp}\not{p}\Phi_V^T(k) + \frac{im_V}{p\cdot n_+}\gamma_5\varepsilon_{\mu\nu\alpha\beta}\gamma^\mu\epsilon^{\perp\nu}p^\alpha n_+^\beta\Phi_V^A(k)\right\}_{ji}, \tag{32}$$

where f_B and f_ψ are the decay constants of the B_u and ψ mesons, respectively. $\epsilon^{\parallel}$ ($\epsilon^{\perp}$) is the longitudinal (transverse) polarization vector. $n_+ = (1,0,0)$ and $n_- = (0,1,0)$ are the positive and negative null light-cone vectors satisfying the conditions of $n_\pm^2 = 0$ and $n_+\cdot n_- = 1$. The chiral parameter μ_P is given by [68]:

$$\mu_P = \frac{m_\pi^2}{m_u + m_d} = \frac{m_K^2}{m_{u,d} + m_s} \approx (1.6\pm0.2)\,{\rm GeV}. \tag{33}$$

According to the twist classification in Refs. [66–70], the WFs of $\Phi_{B,P}^{a}$ and $\Phi_{\psi,V}^{v,T}$ are twist-2, while the WFs of $\Phi_{B,P}^{p,t}$ and $\Phi_{\psi,V}^{t,s,V,A}$ are twist-3. The WFs for the nS and nD psion states are given in Appendix A. In general, these mesonic WFs are the functions of two variables, the longitudinal momentum fractions x_i and the transverse momentum k_{iT} of the valence quarks. It is unanimously assumed with both the QCDF and pQCD approaches that outside the soft regions, the contributions from the transverse momentum can be neglected and the collinear approximation should work well [19–26, 38–47]. One can obtain the corresponding DAs by integrating out the transverse momentum from the WFs. Near the endpoint regions where $x_i \to 0$ or 1, the collinear factorization approximation should no longer be valid [21–24]. The pQCD approach [38–40] suggests that the effects of the transverse momentum cannot be overlooked. In addition, the valence quarks have different momentum fractions and velocities near the endpoint. The hadrons cannot be regarded as color transparent. The Sudakov factors should be introduced for the participating WFs in order to suppress the soft and non-perturbative contributions from the small x_i and the large k_{iT} regions [38–47].

In our calculation, the expressions for the DAs involved are listed as follows [67–74]:

$$\phi_B^p(x) = A{\rm exp}\left\{-\frac{1}{8\omega_1^2}\left(\frac{m_u^2}{x} + \frac{m_b^2}{\bar{x}}\right)\right\}, \tag{34}$$

$$\phi_B^a(x) = B\phi_B^p(x)x\bar{x}, \tag{35}$$

$$\phi_{\psi(1S)}^v(x) = Cx\bar{x}{\rm exp}\left\{-\frac{1}{8\omega_2^2}\left(\frac{m_c^2}{x} + \frac{m_c^2}{\bar{x}}\right)\right\}, \tag{36}$$

$$\phi_{\psi(2S)}^v(x) = D\phi_{\psi(1S)}^v(x)\left\{1 + \frac{m_c^2}{2\omega_2^2 x\bar{x}}\right\}, \tag{37}$$

$$\phi^v_{\psi(3S)}(x)=E\phi^v_{\psi(1S)}(x)\left\{\left(1-\frac{m_c^2}{2\omega_2^2 x\bar{x}}\right)^2+6\right\}, \quad (38)$$

$$\phi^v_{\psi(1D)}(x)=F\phi^v_{\psi(1S)}(x)\left\{1+\frac{m_c^2}{8\omega_2^2 x\bar{x}}\right\}, \quad (39)$$

$$\phi^v_{\psi(2D)}(x)=G\phi^v_{\psi(1S)}(x)\left\{\left(1+\frac{m_c^2}{\omega_2^2 x\bar{x}}\right)^2+15\right\}, \quad (40)$$

$$\phi^t_\psi(x)=H\phi^v_\psi(x)\xi^2/(x\bar{x}), \quad (41)$$

$$\phi^V_\psi(x)=I\phi^v_\psi(x)(1+\xi^2)/(x\bar{x}), \quad (42)$$

$$\phi^T_\psi(x)=J\phi^v_\psi(x), \quad (43)$$

$$\phi^a_P(x)=\mathrm{i}f_P 6x\bar{x}\sum_{i=0}^{n}a_i^P C_i^{3/2}(\xi), \quad (44)$$

$$\phi^v_V(x)=f_V 6x\bar{x}\sum_{i=0}^{n}a_i^{\parallel} C_i^{3/2}(\xi), \quad (45)$$

$$\phi^T_V(x)=f^T_V 6x\bar{x}\sum_{i=0}^{n}a_i^{\perp} C_i^{3/2}(\xi), \quad (46)$$

$$\phi^p_P(x)=+\mathrm{i}f_P C_0^{1/2}(\xi), \quad (47)$$

$$\phi^t_P(x)=-\mathrm{i}f_P C_1^{1/2}(\xi), \quad (48)$$

$$\phi^t_V(x)=+3f^T_V\xi^2, \quad (49)$$

$$\phi^s_V(x)=-3f^T_V\xi, \quad (50)$$

$$\phi^V_V(x)=+\frac{3}{4}f_V(1+\xi^2), \quad (51)$$

$$\phi^A_V(x)=-\frac{3}{2}f_V\xi. \quad (52)$$

where x and $\bar{x}=1-x$ are the momentum fractions of the valence quarks. The variable $\xi=x-\bar{x}$. The parameter ω_i determines the average transverse momentum of partons and $\omega_i\simeq m_i\alpha_s$ [71–77]. The parameters A, $\cdots$, J in Eqs. (34-43) are the normalization coefficients. The DAs of Eqs. (34-43) satisfy the normalization conditions,

$$\int_0^1 \mathrm{d}x\phi^{a,p}_B(x)=1, \quad (53)$$

$$\int_0^1 \mathrm{d}x\phi^{v,t,V,T}_{\psi(nL)}(x)=1. \quad (54)$$

The DAs of Eqs. (44-52) are the normalized expressions. The parameter f_P is the decay constant for the pseudoscalar meson P. The parameters f_V and f_V^T are the longitudinal and transverse decay constants for the vector meson V. The non-perturbative parameters $a_i^{P,\parallel,\perp}$ are the Gegenbauer moments, with $a_0^{P,\parallel,\perp}=1$ for the asymptotic forms. The Gegenbauer polynomials $C_i^j(\xi)$ are expressed as follows:

$$C_0^j(\xi)=1, \quad (55)$$

$$C_1^j(\xi)=2j\xi, \quad (56)$$

$$C_2^j(\xi)=2j(j+1)\xi^2-j, \quad (57)$$

.....

A distinguishing feature of the DAs in Eqs. (34-43) is the exponential functions. These exponential factors are proportional to the ratio of m_i^2/x_i, so that the shape lines of DAs in Eqs. (34-43) are generally consistent with the seemingly plausible suspicion that the momentum fractions x_i are shared by the valence quarks according to the quark mass m_i. In addition, the DAs will approach zero when $x_i\to 0$ and 1, due to the effective cutoff of the endpoint contributions from the exponential functions. The curves of the normalized DAs $\phi_B^{a,p}(x)$ and $\phi_\psi^{v,t,V}(x)$ in Eqs. (34-43) versus the parton momentum fraction x are shown in Fig. 1. It is seen that: (1) the parton momentum fraction of the spectator quark in the B_u meson peaks in the $x<0.4$ region; (2) the DAs of $\phi_\psi^{v,t,V}(x)$ are symmetric with respect to the $x\leftrightarrow\bar{x}$ transformation; and (3) the difference between the DAs for the $2S$ and $1D$ psion states (and the $3S$ and $2D$ psion states) is subtle.

Some properties of the psion resonances are collected in Table 1, where the decay constant f_ψ is defined by $\langle 0|\bar{c}\gamma^\mu c|\psi\rangle = f_\psi m_\psi \epsilon_\psi^\mu$ and can be extracted from the electronic $\psi\to e^+e^-$ decay through the formula including the QCD radiative corrections [48–51, 78–83],

$$\Gamma_{ee}=\Gamma(\psi\to e^+e^-)=\frac{16\pi}{27}\alpha^2_{\rm QED}(m_\psi)\frac{f_\psi^2}{m_\psi}\left\{1-\frac{16}{3\pi}\alpha_s(m_\psi)\right\}, \quad (58)$$

where the RG evolution equation for the coupling $\alpha_{\rm QED}$ (α_s) of the electromagnetic (strong) interactions is given in Ref. [84] (Ref. [4]). In our calculation, the one-loop leptonic contributions to $\alpha_{\rm QED}$ are considered with the initial value $\alpha_{\rm QED}(m_W)=1/128$ resulting in $\alpha_{\rm QED}(m_\psi)\sim 1/131$, and the NLO contributions to the coupling α_s of the strong interactions are considered with the initial value $\alpha_s(m_Z)=0.1182$ [1]. It is seen from Table 1 that there exist differences in the dielectric psion decay widths, which are assumed to be accommodated appropriately with the interferences between the S- and D- states [48–60]. Although with nearly the same shape lines for the $2S$- and $1D$-wave (and the $3S$- and $2D$-wave) psion DAs (see Fig. 1), the differences in the decay constants might have an influence on the $B_u\to\psi M$ decays due to the S-D mixing. In this paper, the S-D wave mixing effects on the $B_u\to\psi M$ decays are investigated. The physical psion mesons are admixtures of the S- and D- states [48–60],

$$\begin{pmatrix}\psi(3686)\\ \psi(3770)\end{pmatrix}=\begin{pmatrix}\cos\theta_1 & \sin\theta_1\\ -\sin\theta_1 & \cos\theta_1\end{pmatrix}\begin{pmatrix}\psi(2S)\\ \psi(1D)\end{pmatrix}, \quad (59)$$

$$\begin{pmatrix}\psi(4040)\\ \psi(4160)\end{pmatrix}=\begin{pmatrix}\cos\theta_2 & \sin\theta_2\\ -\sin\theta_2 & \cos\theta_2\end{pmatrix}\begin{pmatrix}\psi(3S)\\ \psi(2D)\end{pmatrix}, \quad (60)$$

where the subscript i of the S-D mixing angle θ_i corresponds to the radial quantum number n of the $\psi(nD)$ states. There are two sets of possible ranges for the value

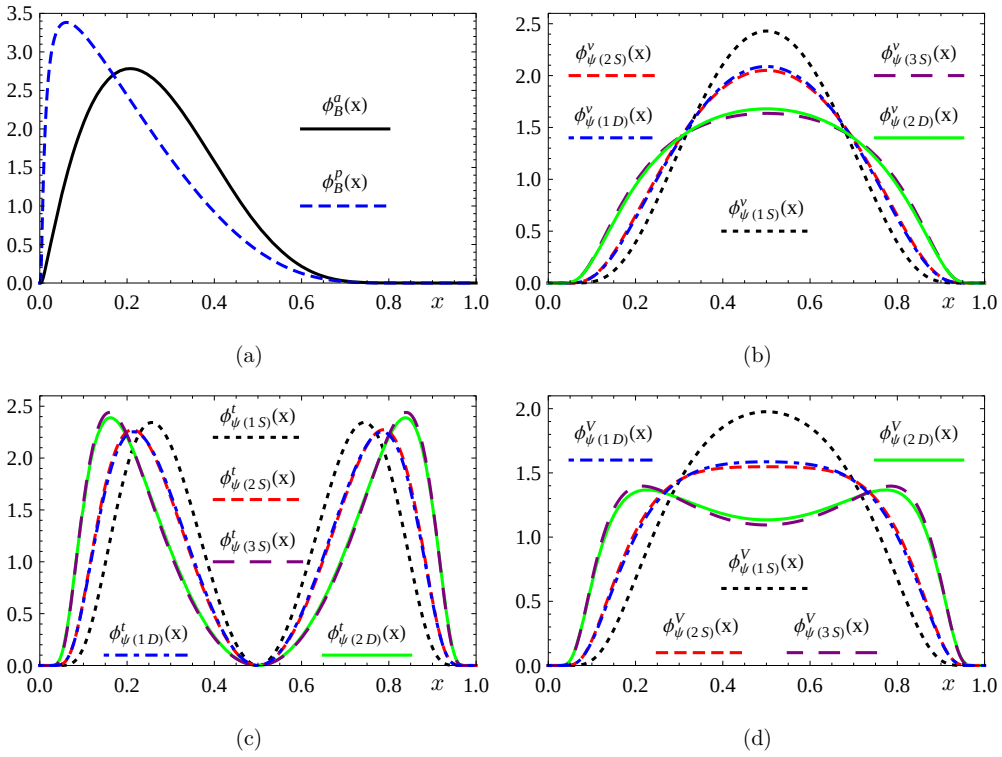

Fig. 1. (color online) The normalized DAs of $\phi_B^{a,p}(x)$ and $\phi_\psi^{v,t,V}(x)$ (vertical axis) versus the parton momentum fraction x (horizontal axis).

Table 1. Some properties of the psion resonances [1], where Γ denotes the full decay width; $\mathcal{B}r_{ee}$ and Γ_{ee} denote the branching ratio and partial width respectively for the pure leptonic $\psi \to e^+e^-$ decay; f_ψ is the decay constant obtained with Eq. (58); and $\alpha_s(m_\psi)$ is the QCD coupling at the scale $\mu = m_\psi$.

meson	mass/MeV	Γ/keV	$\mathcal{B}r_{ee}$	Γ_{ee}/keV	f_ψ/MeV	$\alpha_s(m_\psi)$
$\psi(2S)$	3686.097±0.025	296±8	$(7.89\pm0.17)\times10^{-3}$	2.34±0.04	358.8±3.1	0.227
$\psi(3770)$	3773.13±0.35	$(27.2\pm1.0)\times10^3$	$(9.6\pm0.7)\times10^{-6}$	0.262±0.018	121.2±4.2	0.225
$\psi(4040)$	4039±1	$(80\pm10)\times10^3$	$(1.07\pm0.16)\times10^{-5}$	0.86±0.07	225.4±9.4	0.220
$\psi(4160)$	4191±5	$(70\pm10)\times10^3$	$(6.9\pm3.3)\times10^{-6}$	0.48±0.22	170.9±45.2	0.217

of the $2S$-$1D$ mixing angle [49–58][1)], i.e., $\theta_1 \approx -10^\circ \sim -14^\circ$ and $\theta_1 \approx +25^\circ \sim +30^\circ$. The possible value of the $3S$-$2D$ mixing angle is $\theta_2 \approx -35^\circ$ [50–54]. As an approximation in the numerical computation, the values of $\theta_1 \approx -(12\pm2)^\circ$ and $+(27\pm2)^\circ$ [57] and $\theta_2 \approx -35^\circ$ [51, 52] will be used. The assumed mass relations are $m_{\psi(2S)} \approx m_{\psi(3686)}$, $m_{\psi(1D)} \approx m_{\psi(3770)}$, $m_{\psi(3S)} \approx m_{\psi(4040)}$ and $m_{\psi(2D)} \approx m_{\psi(4160)}$.

2.5 Decay amplitudes

Within the pQCD framework, the Feynman diagrams for the $B_u \to \psi K$ decay are shown in Fig. 2. The spectator quark always interacts with one hard gluon in each subdiagram. The diagrams Fig. 2(a,b) are the factorizable emission topologies, where the gluons are exchanged between the initial B_u meson and the recoil K meson. It is possible to completely isolate the emission psion particle from the B_uK system, and hence the integral of the psion WFs will reduce to the psion decay constant. The diagrams Fig. 2(c,d) are the non-factorizable emission topologies, where the gluons are exchanged between the psion particle and the B_uK system, and hence no meson can escape from the interferences of other mesons. The diagrams Fig. 2(c,d) are also called the spectator scattering topologies with the QCDF approach [20–25]. The non-factorizable HME can be written as the convolution integral of all the participating meson WFs. Compared with the factorizable contributions from Fig. 2(a,b), the non-factorizable contributions from Fig. 2(c,d) are color-suppressed, which is quite similar to the cases between the external and internal W emission topologies.

1) The possible values of the $2S$-$1D$ mixing angle are: $\theta_1 \approx -10^\circ$ and $+30^\circ$ in Ref. [55], $\theta_1 \approx -13^\circ$ and $+26^\circ$ in Ref. [56], $\theta_1 \approx -(12\pm2)^\circ$ and $+(27\pm2)^\circ$ in Ref. [57], $\theta_1 \approx -12^\circ$ and $+25^\circ$ in Ref. [50], and $\theta_1 \approx -11^\circ$ in Ref. [49].

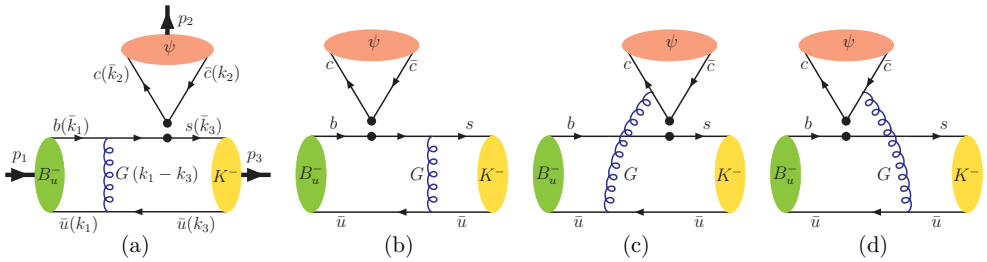

Fig. 2. (color online) The Feynman diagrams for the $B_u^- \to \psi K^-$ decay with the pQCD approach, where (a,b) and (c,d) are factorizable and non-factorizable topologies, respectively.

After a direct calculation, the amplitudes for the $B_u \to \psi M$ decays are written as follows:

$$\begin{aligned}\mathcal{A}(B_u\to\psi P) &= \frac{\pi G_{\rm F} C_{\rm F}}{\sqrt{2}N_c} f_B f_\psi \Big\{ \big(V_{cb}V_{cd}^*\delta_{P,\pi}+V_{cb}V_{cs}^*\delta_{P,K}\big)\Big[a_2\big(\mathcal{A}_{a,P}^{LL}+\mathcal{A}_{b,P}^{LL}\big)+C_1\big(\mathcal{A}_{c,P}^{LL}+\mathcal{A}_{d,P}^{LL}\big)\Big] \\ &-\big(V_{tb}V_{td}^*\delta_{P,\pi}+V_{tb}V_{ts}^*\delta_{P,K}\big)\Big[\big(a_3+a_9\big)\big(\mathcal{A}_{a,P}^{LL}+\mathcal{A}_{b,P}^{LL}\big)+\big(a_5+a_7\big)\big(\mathcal{A}_{a,P}^{LR}+\mathcal{A}_{b,P}^{LR}\big) \\ &+\big(C_4+C_{10}\big)\big(\mathcal{A}_{c,P}^{LL}+\mathcal{A}_{d,P}^{LL}\big)+\big(C_6+C_8\big)\big(\mathcal{A}_{c,P}^{LR}+\mathcal{A}_{d,P}^{LR}\big)\Big]\Big\}, \end{aligned} \tag{61}$$

$$\mathcal{A}(B_u\to\psi V) = \mathcal{A}_L(\epsilon_\psi^\parallel\cdot\epsilon_V^\parallel)+\mathcal{A}_N(\epsilon_\psi^\perp\cdot\epsilon_V^\perp)+{\rm i}\mathcal{A}_T\varepsilon_{\mu\nu\alpha\beta}\epsilon_\psi^\mu\epsilon_V^\nu p_\psi^\alpha p_V^\beta, \tag{62}$$

$$\begin{aligned}\mathcal{A}_i(B_u\to\psi V) &= \frac{\pi G_{\rm F} C_{\rm F}}{\sqrt{2}N_c} f_B f_\psi \Big\{ \big(V_{cb}V_{cd}^*\delta_{V,\rho}+V_{cb}V_{cs}^*\delta_{V,K^*}\big)\Big[a_2\big(\mathcal{A}_{a,i}^{LL}+\mathcal{A}_{b,i}^{LL}\big)+C_1\big(\mathcal{A}_{c,i}^{LL}+\mathcal{A}_{d,i}^{LL}\big)\Big] \\ &-\big(V_{tb}V_{td}^*\delta_{V,\rho}+V_{tb}V_{ts}^*\delta_{V,K^*}\big)\Big[\big(a_3+a_9\big)\big(\mathcal{A}_{a,i}^{LL}+\mathcal{A}_{b,i}^{LL}\big)+\big(a_5+a_7\big)\big(\mathcal{A}_{a,i}^{LR}+\mathcal{A}_{b,i}^{LR}\big) \\ &+\big(C_4+C_{10}\big)\big(\mathcal{A}_{c,i}^{LL}+\mathcal{A}_{d,i}^{LL}\big)+\big(C_6+C_8\big)\big(\mathcal{A}_{c,i}^{LR}+\mathcal{A}_{d,i}^{LR}\big)\Big]\Big\}, \qquad \text{for } i=L,N,T \end{aligned} \tag{63}$$

$$a_i=\begin{cases} C_i+C_{i+1}/N_c, & \text{for odd } i \\ C_i+C_{i-1}/N_c, & \text{for even } i \end{cases} \tag{64}$$

where the color factor $C_{\rm F}=4/3$ and the color number $N_c=3$. For the amplitude building block $\mathcal{A}_{i,j}^k$, the subscript i corresponds to the subdiagram indices of Fig. 2; the subscript $j=P,\,L,\,N,\,T$ denotes the invariant polarization amplitudes, and the superscript k refers to the two possible Dirac structures $\Gamma_1\otimes\Gamma_2$ of the operators $(\bar{q}_1q_2)_{\Gamma_1}(\bar{q}_3q_4)_{\Gamma_2}$, namely $k=LL$ for $(V-A)\otimes(V-A)$ and $k=LR$ for $(V-A)\otimes(V+A)$. The explicit expressions of the building blocks $\mathcal{A}_{i,j}^k$ are collected in Appendix B.

In addition, the amplitudes for the $B_u\to\psi V$ decays are conventionally expressed as the helicity amplitudes. The relation between the helicity amplitudes $H_{0,\parallel,\perp}$ and the scalar amplitudes $\mathcal{A}_{L,N,T}$ is [85–88]:

$$H_0 = \mathcal{A}_L(\epsilon_\psi^\parallel\cdot\epsilon_V^\parallel), \tag{65}$$

$$H_\parallel = \sqrt{2}\mathcal{A}_N, \tag{66}$$

$$H_\perp = \sqrt{2}m_{B_u}p_{\rm cm}\mathcal{A}_T. \tag{67}$$

3 Numerical results and discussion

In the rest frame of the B_u meson, the branching ratios are defined as:

$$\mathcal{B}r(B_u\to\psi P)=\frac{\tau_{B_u}}{8\pi}\frac{p_{\rm cm}}{m_{B_u}^2}|\mathcal{A}(B_u\to\psi P)|^2, \tag{68}$$

$$\mathcal{B}r(B_u\to\psi V)=\frac{\tau_{B_u}}{8\pi}\frac{p_{\rm cm}}{m_{B_u}^2}\Big\{|H_0|^2+|H_\parallel|^2+|H_\perp|^2\Big\}, \tag{69}$$

where $\tau_{B_u}=(1.638\pm0.004)$ ps is the lifetime of the B_u meson [1].

The numerical values of the input parameters are listed in Tables 1 and 2, where their central values are regarded as the default inputs unless otherwise specified. Our numerical results for the branching ratios, together with the experimental data, are presented in Tables 3 and 4. The theoretical uncertainties come from the quark mass m_c and m_b, and the hadronic parameters (including the decay constants, Gegenbauer moments, and the chiral parameter), respectively. Some comments follow.

1) The relation between the CKM parameters $(\rho,\,\eta)$ and $(\bar{\rho},\,\bar{\eta})$ is $(\rho,\,\eta)\simeq(\bar{\rho},\bar{\eta})(1+\lambda^2/2+\cdots)$.

Table 2. The numerical values of the input parameters.

CKM parameters[1)]	$A = 0.811\pm0.026$ [1],	$\lambda = 0.22506\pm0.00050$ [1],
	$\bar{\rho} = 0.124^{+0.019}_{-0.018}$ [1],	$\bar{\eta} = 0.356\pm0.011$ [1],
mass of the particles	$m_{\pi^\pm} = 139.57$ MeV [1],	$m_{K^\pm} = 493.677\pm0.016$ MeV [1],
	$m_\rho = 775.26\pm0.25$ MeV [1],	$m_{K^{*\pm}} = 891.66\pm0.26$ MeV [1],
$m_{B_u} = 5279.31\pm0.15$ MeV [1],	$m_b = 4.78\pm0.06$ GeV [1],	$m_c = 1.67\pm0.07$ GeV [1],
decay constants	$f_\pi = 130.2\pm1.7$ MeV [1],	$f_K = 155.6\pm0.4$ MeV [1],
	$f_\rho = 216\pm3$ MeV [69],	$f_{K^*} = 220\pm5$ MeV [69],
$f_{B_u} = 187.1\pm4.2$ MeV [1],	$f_\rho^T = 165\pm9$ MeV [69],	$f_{K^*}^T = 185\pm10$ MeV [69],
Gegenbauer moments at the scale of $\mu = 1$ GeV		
$a_1^K = -0.06\pm0.03$ [70],	$a_2^K = 0.25\pm0.15$ [70],	$a_2^\pi = 0.25\pm0.15$ [70],
$a_1^{\parallel,K^*} = -0.03\pm0.02$ [69],	$a_2^{\parallel,K^*} = 0.11\pm0.09$ [69],	$a_2^{\parallel,\rho} = 0.15\pm0.07$ [69],
$a_1^{\perp,K^*} = -0.04\pm0.03$ [69],	$a_2^{\perp,K^*} = 0.10\pm0.08$ [69],	$a_2^{\perp,\rho} = 0.14\pm0.06$ [69],

Table 3. The branching ratios for the $B_u \to \psi(2S)M$, $\psi(3770)M$ decays, where the theoretical uncertainties come from the quark mass m_c, m_b, and the hadronic parameters, respectively. The numbers in the parentheses are the results without the non-factorizable contributions.

final states	unit	data [1]	$\theta_1 = 0$	$\theta_1 = -12^\circ$	$\theta_1 = +27^\circ$
$\psi(2S)K^-$	10^{-4}	6.26±0.24	$11.77^{+0.22+1.92+4.99}_{-0.24-1.59-3.88}$	$9.67^{+0.18+1.57+4.18}_{-0.20-1.29-3.22}$	$12.93^{+0.24+2.12+5.65}_{-0.26-1.79-4.35}$
			$(13.24^{+0.00+2.08+5.38}_{-0.00-1.73-4.22})$	$(10.87^{+0.00+1.70+4.51}_{-0.00-1.40-3.51})$	$(14.56^{+0.00+2.30+6.11}_{-0.00-1.95-4.75})$
$\psi(2S)\pi^-$	10^{-5}	2.44±0.30	$1.91^{+0.05+0.42+0.87}_{-0.05-0.34-0.66}$	$1.56^{+0.04+0.35+0.72}_{-0.04-0.28-0.55}$	$2.10^{+0.05+0.46+0.99}_{-0.06-0.37-0.74}$
			$(2.13^{+0.00+0.46+0.92}_{-0.00-0.37-0.71})$	$(1.74^{+0.00+0.37+0.77}_{-0.00-0.30-0.59})$	$(2.35^{+0.00+0.50+1.06}_{-0.00-0.41-0.80})$
$\psi(3770)K^-$	10^{-4}	4.9±1.3	$1.34^{+0.03+0.23+0.69}_{-0.03-0.21-0.50}$	$3.33^{+0.06+0.56+1.60}_{-0.07-0.50-1.19}$	$0.24^{+0.00+0.04+0.16}_{-0.01-0.02-0.10}$
			$(1.51^{+0.00+0.25+0.75}_{-0.00-0.23-0.55})$	$(3.77^{+0.00+0.61+1.74}_{-0.00-0.55-1.31})$	$(0.26^{+0.00+0.05+0.17}_{-0.00-0.02-0.11})$
$\psi(3770)\pi^-$	10^{-6}	—	$2.24^{+0.06+0.49+1.26}_{-0.07-0.39-0.88}$	$5.53^{+0.14+1.22+2.87}_{-0.16-0.97-2.08}$	$0.37^{+0.01+0.08+0.25}_{-0.01-0.07-0.16}$
			$(2.50^{+0.00+0.54+1.35}_{-0.00-0.43-0.96})$	$(6.17^{+0.00+1.32+3.08}_{-0.00-1.06-2.26})$	$(0.40^{+0.00+0.09+0.27}_{-0.00-0.07-0.17})$
$\psi(2S)K^{*-}$	10^{-4}	6.7±1.4	$12.88^{+0.44+2.11+4.05}_{-0.63-2.01-3.31}$	$10.72^{+0.35+1.61+3.43}_{-0.54-1.75-2.79}$	$13.80^{+0.51+2.60+4.52}_{-0.65-1.94-3.65}$
			$(9.76^{+0.00+1.91+3.14}_{-0.00-1.78-2.47})$	$(8.12^{+0.00+1.47+2.66}_{-0.00-1.55-2.08})$	$(10.47^{+0.00+2.36+3.51}_{-0.00-1.72-2.73})$
$\psi(2S)\rho^-$	10^{-5}	—	$4.46^{+0.25+0.87+1.06}_{-0.21-0.75-0.91}$	$3.67^{+0.21+0.71+0.89}_{-0.17-0.62-0.76}$	$4.89^{+0.26+0.96+1.24}_{-0.23-0.83-1.04}$
			$(3.43^{+0.00+0.80+0.79}_{-0.00-0.67-0.69})$	$(2.81^{+0.00+0.65+0.66}_{-0.00-0.55-0.58})$	$(3.79^{+0.00+0.88+0.93}_{-0.00-0.75-0.80})$
$\psi(3770)K^{*-}$	10^{-4}	—	$1.20^{+0.06+0.42+0.50}_{-0.04-0.05-0.37}$	$3.21^{+0.15+0.88+1.20}_{-0.13-0.29-0.93}$	$0.36^{+0.00+0.00+0.16}_{-0.03-0.12-0.12}$
			$(0.92^{+0.00+0.38+0.39}_{-0.00-0.05-0.28})$	$(2.45^{+0.00+0.79+0.93}_{-0.00-0.26-0.70})$	$(0.26^{+0.00+0.00+0.12}_{-0.00-0.10-0.09})$
$\psi(3770)\rho^-$	10^{-6}	—	$4.93^{+0.17+1.02+1.69}_{-0.20-0.87-1.30}$	$12.35^{+0.53+2.49+3.74}_{-0.53-2.14-2.99}$	$0.92^{+0.10+0.16+0.38}_{-0.05-0.14-0.30}$
			$(3.95^{+0.00+0.95+1.32}_{-0.00-0.79-1.02})$	$(9.76^{+0.00+2.32+2.87}_{-0.00-1.94-2.31})$	$(0.65^{+0.00+0.14+0.26}_{-0.00-0.12-0.20})$

(1) It has been shown in Refs. [22–24] that the contributions from the spectator scattering topologies to the coefficient a_2 with the QCDF approach are amplified by the large Wilson coefficient C_1, and the contributions are notable for the $B \to J/\psi M$ decays [9, 17]. Hence, it is initially expected that the non-factorizable contributions from Fig. 2(c,d) should be significant for the $B_u \to \psi M$ decays. However, it is seen from the numbers in Tables 3 and 4 that compared with the factorizable contributions, the non-factorizable contributions to the branching ratios are important, but not so obvious as expected. One of the reasons might be that the opposite signs of the charm quark propagators of Fig. 2(c) and Fig. 2(d) results in destructive interference between their amplitudes. In addition, the amplitudes of Fig. 2(c,d) are suppressed by the color factor $1/N_c$ relative to the amplitudes of Fig. 2(a,b) (see the expressions listed in Appendix B). It is also shown that the non-factorizable contributions are positive (negative) to branching ratios for the $B_u \to \psi V$ (ψP) decays.

(2) The $B_u \to \psi(2S)M$ decays have been studied with the pQCD approach in Refs. [15, 16], by considering part of the NLO factorizable vertex corrections, but without the $2S$-$1D$ mixing effects on psions. Our numerical results generally agree with those of Refs. [15, 16] within theoretical uncertainties, although with different param-

Table 4. The branching ratios for the $B_u \to \psi(4040)M$, $\psi(4160)M$ decays, where the theoretical uncertainties come from the quark mass m_c, m_b, and the hadronic parameters, respectively. The numbers in the parentheses are the results without the non-factorizable contributions.

final states	unit	data [1]	$\theta_2 = 0$	$\theta_2 = -35°$
$\psi(4040)K^-$	10^{-4}	<1.3	$4.21^{+0.06+0.77+2.55}_{-0.05-0.58-1.77}$	$0.52^{+0.01+0.09+1.07}_{-0.01-0.07-0.41}$
			$(5.08^{+0.00+0.86+2.91}_{-0.00-0.66-2.06})$	$(0.61^{+0.00+0.10+1.24}_{-0.00-0.08-0.49})$
$\psi(4040)\pi^-$	10^{-6}	—	$7.84^{+0.21+1.77+5.16}_{-0.17-1.30-3.49}$	$0.85^{+0.03+0.21+2.00}_{-0.02-0.16-0.71}$
			$(9.47^{+0.00+1.99+6.02}_{-0.00-1.47-4.10})$	$(1.00^{+0.00+0.23+2.36}_{-0.00-0.18-0.84})$
$\psi(4160)K^-$	10^{-4}	5.1 ± 2.7	$2.21^{+0.03+0.42+3.07}_{-0.02-0.30-1.47}$	$5.41^{+0.08+1.02+5.36}_{-0.06-0.74-3.00}$
			$(2.72^{+0.00+0.48+3.63}_{-0.00-0.34-1.78})$	$(6.59^{+0.00+1.14+6.26}_{-0.00-0.84-3.57})$
$\psi(4160)\pi^-$	10^{-6}	—	$4.65^{+0.12+1.00+6.87}_{-0.09-0.70-3.15}$	$10.88^{+0.28+2.40+11.64}_{-0.22-1.72-6.26}$
			$(5.71^{+0.00+1.13+8.16}_{-0.00-0.80-3.83})$	$(13.25^{+0.00+2.70+13.75}_{-0.00-1.95-7.51})$
$\psi(4040)K^{*-}$	10^{-4}	—	$2.97^{+0.03+0.71+1.61}_{-0.05-0.62-1.10}$	$0.75^{+0.00+0.23+0.80}_{-0.01-0.20-0.39}$
			$(2.17^{+0.00+0.62+1.26}_{-0.00-0.53-0.84})$	$(0.58^{+0.00+0.21+0.61}_{-0.00-0.18-0.29})$
$\psi(4040)\rho^-$	10^{-5}	—	$1.52^{+0.02+0.16+0.64}_{-0.02-0.28-0.47}$	$0.26^{+0.00+0.02+0.33}_{-0.00-0.14-0.16}$
			$(1.19^{+0.00+0.15+0.53}_{-0.00-0.26-0.38})$	$(0.21^{+0.00+0.02+0.26}_{-0.00-0.12-0.13})$
$\psi(4160)K^{*-}$	10^{-4}	—	$0.69^{+0.01+0.37+0.92}_{-0.01-0.28-0.43}$	$2.32^{+0.03+0.87+2.05}_{-0.04-0.67-1.15}$
			$(0.47^{+0.00+0.31+0.68}_{-0.00-0.22-0.30})$	$(1.63^{+0.00+0.76+1.55}_{-0.00-0.57-0.84})$
$\psi(4160)\rho^-$	10^{-5}	—	$0.56^{+0.01+0.15+0.66}_{-0.00-0.11-0.34}$	$1.57^{+0.02+0.18+1.21}_{-0.01-0.30-0.73}$
			$(0.43^{+0.00+0.13+0.54}_{-0.00-0.10-0.27})$	$(1.21^{+0.00+0.16+0.99}_{-0.00-0.26-0.58})$

eters. In the future, a careful and comprehensive study of the NLO corrections to the $B \to \psi M$ decays is desperately needed, and will be essential for forthcoming precision measurements at the LHCb and Belle-II experiments.

(3) The S-D wave mixture has literally altered the branching ratios for the $B_u \to \psi M$ decays. The $B_u \to \psi(2S)K^{(*)}$, $\psi(3770)K$, $\psi(4160)K$, $\psi(2S)\pi$ decays can be reasonably accommodated within theoretical uncertainties with the appropriate S-D wave mixing angles and other inputs. The angle θ_1 for $2S$-$1D$ mixing and θ_2 for $3S$-$2D$ mixing prefer the negative values, except for the $B_u \to \psi(2S)\pi$ decay. However, the current experimental data for $B_u \to \psi M$ decays cannot offer the S-D mixing angles (θ_1 and θ_2) with a severe constraint (also see Fig. 3). With the successful implementation of the high-luminosity LHCb and SuperKEKB experiments, more accurate measurements of the $B \to \psi M$ decays will be obtained. In addition, a comprehensive study with more processes pertinent to the psions, including the pure leptonic psion decays and the $B \to \psi M$ decays, are necessary to determine the S-D wave mixing angles in the future.

(4) The excited psions with a large mass will certainly carry a large portion of energy in the B meson decay when they are emitted from the interaction point. It is therefore natural to doubt whether the gluons exchanged between the B meson and the recoiled M meson are hard enough to validate the perturbative calculation and the practicability of the pQCD approach. In addition, it is shown in Ref. [14] that the variation of the renormalization scale has a great impact on the color-suppressed $B \to J/\psi M$, $\eta_c M$ decays. In order to clear these doubts, it is necessary to check how many shares come from the perturbative domain. The $\psi(4160)$ meson has the largest mass among the psions concerned. To make the analysis more persuasive, we take the $B_u \to \psi(4160)K^*$ decay as an example. The percentage contributions to the branching ratio from different α_s/π regions are shown in Fig. 4. It is seen that more than 60% of contributions come from the $\alpha_s/\pi \leq 0.4$ regions. Our study also shows that more than 80% of contributions to the $B_u \to \psi(2S)\pi$ decay come from the $\alpha_s/\pi \leq 0.4$ regions. These facts imply that the perturbative calculation with the pQCD approach might be feasible. Besides the suppression of the soft contributions from both the Sudakov factors and the exponential functions of DAs in Eqs. (34-43), the choice of the renormalization scale as the maximum among all possible virtualities (see Eq. (B37)) is also an important factor to further ensure the perturbative calculation with the pQCD approach.

(5) Because of the large mass of the excited psions, the phase space for the $B_u \to \psi M$ decays is relatively compact. For example, the total kinetic energy of the final states for the $B_u \to \psi(4160)K^*$ decay is $m_{B_u} - m_\psi - m_M < 200$ MeV. Hence, the final state interactions (FSIs) might have a non-negligible influence on the $B_u \to \psi M$ decays. Overlooking FSIs might be one reason why the QCDF approach is not good enough for the $B \to J/\psi M$ decays in Refs. [17, 18]. The potential FSIs

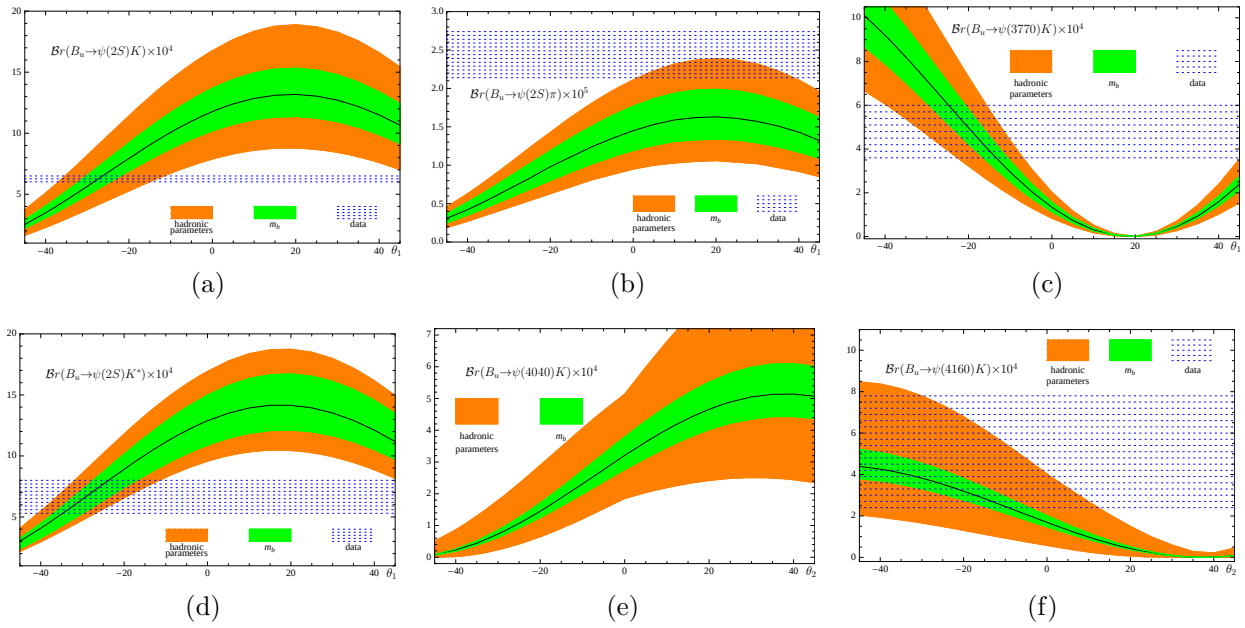

Fig. 3. (color online) The branching ratios (vertical axis) versus the S-D mixing angle (horizontal axis, in degrees). The solid lines denote the results calculated with the default inputs; the dotted blocks denote the current experimental data within one standard error; and the green and orange blocks correspond to theoretical uncertainties from m_b and hadronic parameters, respectively.

deserve much attention for the non-leptonic $B\to\psi M$ decays, but this is beyond the scope of this paper.

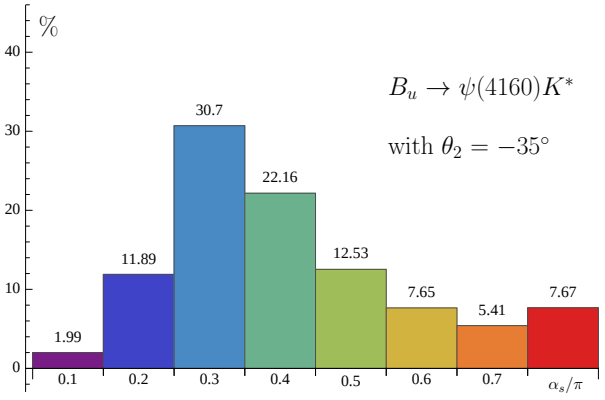

Fig. 4. (color online) The percentage contribution to branching ratio for the $B_u\to\psi(4160)K^*$ decay versus α_s/π, where the numbers above the histogram denote the percentage.

(6) There are lots of theoretical uncertainties, especially from m_b, hadronic parameters and the S-D mixing angles. It is shown in Refs. [12–15] that the pQCD results are sensitive to the model of mesonic WFs/DAs and input parameters. Besides, many other factors, such as FSIs, different models for mesonic WFs/DAs, higher order corrections to HMEs, and so on, are not scrutinized here, in spite of the value of dedicated study. Most of the theoretical uncertainties actually result from our inadequate comprehension of the long-distance and non-perturbative dynamics. Great efforts should be made to improve the reliability of theoretical results.

4 Summary

The color-suppressed non-leptonic $B_u\to\psi M$ decay provides an important place to explore the S-D wave mixing among psions, and test the QCD-inspired approaches for dealing with the hadronic matrix elements. In this paper, the $B_u\to\psi M$ decays are investigated with the pQCD approach, including the contributions of factorizable and non-factorizable emission topologies. We also consider the effects of $2S$-$1D$ and $3S$-$2D$ mixing on psions. It is found that with appropriate inputs, there is generally agreement with the experimental data for the branching ratios for the $B_u\to\psi K$ decays within theoretical uncertainties. However, due to the large experimental and theoretical uncertainties, the angle θ_1 (θ_2) for the $2S$-$1D$ ($3S$-$2D$) wave mixing cannot be determined properly for the moment.

We thank Ms. Nan Li (HNU) for polishing this paper.

Appendix A: Wave functions for the nS and nD charmonium states

The charmonium systems are usually assumed to be nonrelativistic, and their wave functions can be obtained from the solutions of the time-independent Schrödinger equation. Here, we will take the conventional notation to specify the $\psi(nL)$ states, where $n = 1, 2, 3, \cdots$ is the radial quantum number, and the orbital angular momentum $L = 0, 1, 2 \cdots$ corresponds to S, P, $D \cdots$ waves, respectively. The wave functions for the nS and nD states associated with the isotropic linear harmonic oscillator potential are written as follows:

$$\psi_{1S}(\vec{k}) \sim \mathrm{e}^{-\frac{\vec{k}^2}{2\omega^2}}, \tag{A1}$$

$$\psi_{2S}(\vec{k}) \sim \mathrm{e}^{-\frac{\vec{k}^2}{2\omega^2}}(2\vec{k}^2-3\omega^2), \tag{A2}$$

$$\psi_{3S}(\vec{k}) \sim \mathrm{e}^{-\frac{\vec{k}^2}{2\omega^2}}(4\vec{k}^4-20\vec{k}^2\omega^2-15\omega^4), \tag{A3}$$

$$\psi_{1D}(\vec{k}) \sim \vec{k}^2\mathrm{e}^{-\frac{\vec{k}^2}{2\omega^2}}, \tag{A4}$$

$$\psi_{2D}(\vec{k}) \sim \vec{k}^2\mathrm{e}^{-\frac{\vec{k}^2}{2\omega^2}}(2\vec{k}^2-7\omega^2), \tag{A5}$$

where the parameter ω determines the average transverse momentum of the oscillator, i.e., $\langle 1S|\vec{k}_T^2|1S\rangle = \omega^2$. With the power counting rules of the nonrelativistic QCD effective theory [75–77], the characteristic velocity v of the valence quark in heavy quarkonium is about $v \sim \alpha_s$. The parameter $\omega \simeq m\alpha_s$ is taken for the psions in our calculation, where α_s is the QCD coupling constant. We adopt the light-cone momentum and employ the commonly used substitution [89],

$$\vec{k}^2 \to \frac{1}{4}\sum_i \frac{\vec{k}_{iT}^2+m_{q_i}^2}{x_i}, \tag{A6}$$

where x_i, $\vec{k}_{iT}$, m_{q_i} are the longitudinal momentum fraction, transverse momentum, and mass of the valence quark. These variables satisfy the relations $\sum x_i = 1$ and $\sum \vec{k}_{iT} = 0$. After integrating out $\vec{k}_{iT}$ and combining the results with their asymptotic forms [68–70], one can obtain the distribution amplitudes of Eqs. (36-43) for the charmonium states.

Appendix B: Amplitude building blocks for the $B_u^- \to \psi M$ decays

$$\begin{aligned}\mathcal{A}_{a,P}^{LL,LR} = & \int_0^1 \mathrm{d}x_1 \int_0^1 \mathrm{d}x_3 \int_0^\infty b_1 \mathrm{d}b_1 \int_0^\infty b_3 \mathrm{d}b_3 H_f(\alpha,\beta_a,b_1,b_3) E_f(t_a)\alpha_s(t_a) \\ & \times \Big\{ \phi_B^a(x_1) \Big[2m_1 p\{\phi_P^a(x_3)(m_1^2\bar{x}_3+m_2^2 x_3)+m_b\mu_P\phi_P^p(x_3)\} \\ & + t m_b \mu_P \phi_P^t(x_3) \Big] - 2m_1 \phi_B^p(x_1) \Big[2m_1 p m_b \phi_P^a(x_3) \\ & + 2m_1 p \mu_P \phi_P^p(x_3)\bar{x}_3 + \mu_P \phi_P^t(x_3)(t-s x_3) \Big] \Big\},\end{aligned} \tag{B1}$$

$$\begin{aligned}\mathcal{A}_{a,L}^{LL,LR} = & \int_0^1 \mathrm{d}x_1 \int_0^1 \mathrm{d}x_3 \int_0^\infty b_1 \mathrm{d}b_1 \int_0^\infty b_3 \mathrm{d}b_3 H_f(\alpha,\beta_a,b_1,b_3) E_f(t_a)\alpha_s(t_a) \\ & \times \Big\{ 2m_1 \phi_B^p(x_1) \Big[\phi_V^s(x_3) 2m_1 m_3 p \bar{x}_3 + \phi_V^t(x_3) m_3 (t - s x_3) \\ & + \phi_V^v(x_3) m_b s \Big] - \phi_B^a(x_1) \Big[\phi_V^v(x_3)(m_1^2 s \bar{x}_3 + m_2^2 u x_3) \\ & + \phi_V^t(x_3) m_3 m_b t + \phi_V^s(x_3) 2m_1 p m_3 m_b \Big] \Big\},\end{aligned} \tag{B2}$$

$$\begin{aligned}\mathcal{A}_{a,N}^{LL,LR} = & \int_0^1 \mathrm{d}x_1 \int_0^1 \mathrm{d}x_3 \int_0^\infty b_1 \mathrm{d}b_1 \int_0^\infty b_3 \mathrm{d}b_3 H_f(\alpha,\beta_a,b_1,b_3) E_f(t_a)\alpha_s(t_a) \\ & \times \Big\{ \phi_B^p(x_1) 2m_1 m_2 \Big[\phi_V^V(x_3) 2m_3 m_b + \phi_V^T(x_3)(u - 2m_3^2 x_3) \Big] \\ & - \phi_B^a(x_1) \Big[\phi_V^V(x_3) m_2 m_3 (2m_1^2 - u x_3) + \phi_V^T(x_3) m_2 m_b u \\ & + \phi_V^A(x_3) 2m_1 m_2 m_3 p x_3 \Big] \Big\},\end{aligned} \tag{B3}$$

$$\mathcal{A}^{LL,LR}_{a,T} = \int_0^1 \mathrm{d}x_1 \int_0^1 \mathrm{d}x_3 \int_0^\infty b_1 \mathrm{d}b_1 \int_0^\infty b_3 \mathrm{d}b_3 H_f(\alpha,\beta_a,b_1,b_3) E_f(t_a) \alpha_s(t_a) \times m_2 \Big\{ \phi^a_B(x_1) \Big[m_3/(m_1 p) \phi^A_V(x_3)(2m_1^2 - u x_3) + \phi^T_V(x_3) 2m_b + \phi^V_V(x_3) 2m_3 x_3 \Big] - 4\phi^p_B(x_1) \Big[\phi^T_V(x_3) m_1 + \phi^A_V(x_3) m_3 m_b/p \Big] \Big\}, \tag{B4}$$

$$\mathcal{A}^{LL,LR}_{b,P} = 2m_1 p \int_0^1 \mathrm{d}x_1 \int_0^1 \mathrm{d}x_3 \int_0^\infty b_1 \mathrm{d}b_1 \int_0^\infty b_3 \mathrm{d}b_3 H_f(\alpha,\beta_b,b_3,b_1) E_f(t_b) \alpha_s(t_b) \times \Big\{ \phi^a_B(x_1) \phi^a_P(x_3)(m_3^2 \bar{x}_1 + m_2^2 x_1) - \phi^p_B(x_1) \phi^p_P(x_3) 2m_1 \mu_P \bar{x}_1 \Big\}, \tag{B5}$$

$$\mathcal{A}^{LL,LR}_{b,L} = \int_0^1 \mathrm{d}x_1 \int_0^1 \mathrm{d}x_3 \int_0^\infty b_1 \mathrm{d}b_1 \int_0^\infty b_3 \mathrm{d}b_3 H_f(\alpha,\beta_b,b_3,b_1) E_f(t_b) \alpha_s(t_b) \times \Big\{ \phi^a_B(x_1) \phi^v_V(x_3)(m_3^2 t \bar{x}_1 - m_2^2 u x_1) + \phi^p_B(x_1) \phi^s_V(x_3) 4m_1^2 m_3 p \bar{x}_1 \Big\}, \tag{B6}$$

$$\mathcal{A}^{LL,LR}_{b,N} = m_2 m_3 \int_0^1 \mathrm{d}x_1 \int_0^1 \mathrm{d}x_3 \int_0^\infty b_1 \mathrm{d}b_1 \int_0^\infty b_3 \mathrm{d}b_3 H_f(\alpha,\beta_b,b_3,b_1) E_f(t_b) \times \alpha_s(t_b) \phi^a_B(x_1) \Big\{ \phi^V_V(x_3)(u - 2m_1^2 x_1) + \phi^A_V(x_3) 2m_1 p \Big\}, \tag{B7}$$

$$\mathcal{A}^{LL,LR}_{b,T} = -m_2 m_3 \int_0^1 \mathrm{d}x_1 \int_0^1 \mathrm{d}x_3 \int_0^\infty b_1 \mathrm{d}b_1 \int_0^\infty b_3 \mathrm{d}b_3 H_f(\alpha,\beta_b,b_3,b_1) E_f(t_b) \times \alpha_s(t_b) \phi^a_B(x_1) \Big\{ 2\phi^V_V(x_3) + \phi^A_V(x_3)(u - 2m_1^2 x_1)/(m_1 p) \Big\}, \tag{B8}$$

$$\mathcal{A}^{LL}_{c,P} = \frac{1}{N_c} \int_0^1 \mathrm{d}x_1 \int_0^1 \mathrm{d}x_2 \int_0^1 \mathrm{d}x_3 \int_0^\infty \mathrm{d}b_1 \int_0^\infty b_2 \mathrm{d}b_2 \int_0^\infty b_3 \mathrm{d}b_3 H_n(\alpha,\beta_c,b_2,b_3) \times E_n(t_c) \Big\{ \phi^a_B(x_1) \phi^a_P(x_3) 2m_1 p \Big[\phi^v_\psi(x_2) \{ u(x_1 - x_3) + s(x_3 - \bar{x}_2) \} - \phi^t_\psi(x_2) m_2 m_c \Big] + \phi^p_B(x_1) \phi^v_\psi(x_2) m_1 \mu_P \Big[\phi^p_P(x_3) 2m_1 p (x_3 - x_1) + \phi^t_P(x_3) \{ t(x_1 - \bar{x}_2) + s(\bar{x}_2 - x_3) \} \Big] \Big\} \alpha_s(t_c) \delta(b_1 - b_3), \tag{B9}$$

$$\mathcal{A}^{LL}_{c,L} = \frac{1}{N_c} \int_0^1 \mathrm{d}x_1 \int_0^1 \mathrm{d}x_2 \int_0^1 \mathrm{d}x_3 \int_0^\infty \mathrm{d}b_1 \int_0^\infty b_2 \mathrm{d}b_2 \int_0^\infty b_3 \mathrm{d}b_3 H_n(\alpha,\beta_c,b_2,b_3) \times \Big\{ \phi^a_B(x_1) \phi^v_V(x_3) \Big[\phi^v_\psi(x_2) 4m_1^2 p^2 (\bar{x}_2 - x_1) + \phi^t_\psi(x_2) m_2 m_c u \Big] + \phi^p_B(x_1) \phi^v_\psi(x_2) m_1 m_3 \Big[\phi^t_V(x_3) \{ t(\bar{x}_2 - x_1) + s(x_3 - \bar{x}_2) \} + \phi^s_V(x_3) 2m_1 p (x_1 - x_3) \Big] \Big\} E_n(t_c) \alpha_s(t_c) \delta(b_1 - b_3), \tag{B10}$$

$$\mathcal{A}^{LL}_{c,N} = \frac{1}{N_c} \int_0^1 \mathrm{d}x_1 \int_0^1 \mathrm{d}x_2 \int_0^1 \mathrm{d}x_3 \int_0^\infty \mathrm{d}b_1 \int_0^\infty b_2 \mathrm{d}b_2 \int_0^\infty b_3 \mathrm{d}b_3 H_n(\alpha,\beta_c,b_2,b_3) \times E_n(t_c) \delta(b_1 - b_3) \Big\{ \phi^a_B(x_1) \phi^T_\psi(x_2) m_3 m_c \Big[\phi^V_V(x_3) t - \phi^A_V(x_3) 2m_1 p \Big] + \phi^p_B(x_1) \phi^V_\psi(x_2) \phi^T_V(x_3) m_1 m_2 \Big[u(x_3 - x_1) + s(\bar{x}_2 - x_3) \Big] \Big\} \alpha_s(t_c), \tag{B11}$$

$$\begin{aligned}\mathcal{A}^{LL}_{c,T} &= \frac{1}{N_c}\int_0^1\mathrm{d}x_1\int_0^1\mathrm{d}x_2\int_0^1\mathrm{d}x_3\int_0^\infty\mathrm{d}b_1\int_0^\infty b_2\mathrm{d}b_2\int_0^\infty b_3\mathrm{d}b_3 H_n(\alpha,\beta_c,b_2,b_3)\\ &\times\ \delta(b_1-b_3)\Big\{\phi^a_B(x_1)\phi^T_\psi(x_2)m_3m_c\Big[2\phi^V_V(x_3)-\phi^A_V(x_3)t/(m_1p)\Big]\\ &+\ \phi^p_B(x_1)\phi^V_\psi(x_2)\phi^T_V(x_3)2m_1m_2(x_1-\bar{x}_2)\Big\}E_n(t_c)\alpha_s(t_c),\end{aligned}\tag{B12}$$

$$\begin{aligned}\mathcal{A}^{LR}_{c,P} &= \frac{1}{N_c}\int_0^1\mathrm{d}x_1\int_0^1\mathrm{d}x_2\int_0^1\mathrm{d}x_3\int_0^\infty\mathrm{d}b_1\int_0^\infty b_2\mathrm{d}b_2\int_0^\infty b_3\mathrm{d}b_3\delta(b_1-b_3)H_n(\alpha,\beta_c,b_2,b_3)\\ &\times\ \Big\{\phi^a_B(x_1)\phi^a_P(x_3)2m_1p\Big[\phi^v_\psi(x_2)\{u(x_1-x_3)+t(x_1-\bar{x}_2)\}+\phi^t_\psi(x_2)m_2m_c\Big]\\ &+\ \phi^p_B(x_1)\phi^v_\psi(x_2)m_1\mu_P\Big[\phi^p_P(x_3)2m_1p(x_3-x_1)-\phi^t_P(x_3)\{t(x_1-\bar{x}_2)\\ &\quad+s(\bar{x}_2-x_3)\}\Big]-\phi^p_B(x_1)\phi^t_\psi(x_2)\phi^t_P(x_3)4m_1m_2m_c\mu_P\Big\}E_n(t_c)\alpha_s(t_c),\end{aligned}\tag{B13}$$

$$\begin{aligned}\mathcal{A}^{LR}_{c,L} &= \frac{1}{N_c}\int_0^1\mathrm{d}x_1\int_0^1\mathrm{d}x_2\int_0^1\mathrm{d}x_3\int_0^\infty\mathrm{d}b_1\int_0^\infty b_2\mathrm{d}b_2\int_0^\infty b_3\mathrm{d}b_3\delta(b_1-b_3)H_n(\alpha,\beta_c,b_2,b_3)\\ &\times\ \Big\{\phi^a_B(x_1)\phi^v_V(x_3)\Big[\phi^v_\psi(x_2)s\{t(\bar{x}_2-x_1)+u(x_3-x_1)\}-\phi^t_\psi(x_2)m_2m_cu\Big]\\ &+\ \phi^p_B(x_1)\phi^v_\psi(x_2)m_1m_3\Big[\phi^s_V(x_3)2m_1p(x_1-x_3)+\phi^t_V(x_3)\{t(x_1-\bar{x}_2)\\ &+\ s(\bar{x}_2-x_3)\}\Big]+\phi^p_B(x_1)\phi^t_\psi(x_2)\phi^t_V(x_3)m_1m_3(t-s)\frac{2m_c}{m_2}\Big\}E_n(t_c)\alpha_s(t_c),\end{aligned}\tag{B14}$$

$$\begin{aligned}\mathcal{A}^{LR}_{c,N} &= \frac{1}{N_c}\int_0^1\mathrm{d}x_1\int_0^1\mathrm{d}x_2\int_0^1\mathrm{d}x_3\int_0^\infty\mathrm{d}b_1\int_0^\infty b_2\mathrm{d}b_2\int_0^\infty b_3\mathrm{d}b_3\delta(b_1-b_3)H_n(\alpha,\beta_c,b_2,b_3)\\ &\times\ \Big\{\phi^p_B(x_1)\phi^T_V(x_3)m_1\Big[\phi^V_\psi(x_2)m_2\{u(x_1-x_3)+s(x_3-\bar{x}_2)\}+\phi^T_\psi(x_2)2m_cs\Big]\\ &+\ \phi^a_B(x_1)\Big[\phi^V_\psi(x_2)\phi^V_V(x_3)2m_2m_3\{t(\bar{x}_2-x_1)+u(x_3-x_1)\}\\ &-\ \phi^T_\psi(x_2)m_3m_c\{\phi^V_V(x_3)t+\phi^A_V(x_3)2m_1p\}\Big]\Big\}E_n(t_c)\alpha_s(t_c),\end{aligned}\tag{B15}$$

$$\begin{aligned}\mathcal{A}^{LR}_{c,T} &= \frac{1}{N_c}\int_0^1\mathrm{d}x_1\int_0^1\mathrm{d}x_2\int_0^1\mathrm{d}x_3\int_0^\infty\mathrm{d}b_1\int_0^\infty b_2\mathrm{d}b_2\int_0^\infty b_3\mathrm{d}b_3 H_n(\alpha,\beta_c,b_2,b_3)E_n(t_c)\\ &\times\ \delta(b_1-b_3)\Big\{\phi^p_B(x_1)\phi^T_V(x_3)2m_1\Big[\phi^V_\psi(x_2)m_2(\bar{x}_2-x_1)-\phi^T_\psi(x_2)2m_c\Big]\\ &+\ \phi^a_B(x_1)\phi^V_\psi(x_2)\phi^A_V(x_3)\frac{2m_2m_3}{m_1p}\{u(x_1-x_3)+t(x_1-\bar{x}_2)\}\\ &+\ \phi^a_B(x_1)\phi^T_\psi(x_2)2m_3m_c\Big[\phi^V_V(x_3)+\phi^A_V(x_3)\frac{t}{2m_1p}\Big]\Big\}\alpha_s(t_c),\end{aligned}\tag{B16}$$

$$\begin{aligned}\mathcal{A}^{LL}_{d,P} &= \frac{1}{N_c}\int_0^1\mathrm{d}x_1\int_0^1\mathrm{d}x_2\int_0^1\mathrm{d}x_3\int_0^\infty\mathrm{d}b_1\int_0^\infty b_2\mathrm{d}b_2\int_0^\infty b_3\mathrm{d}b_3\delta(b_1-b_3)H_n(\alpha,\beta_d,b_2,b_3)\\ &\times\ \Big\{\phi^a_B(x_1)\phi^a_P(x_3)2m_1p\Big[\phi^v_\psi(x_2)\{u(x_3-x_1)+t(x_2-x_1)\}-\phi^t_\psi(x_2)m_2m_c\Big]\\ &+\ \phi^p_B(x_1)\phi^v_\psi(x_2)m_1\mu_P\Big[\phi^p_P(x_3)2m_1p(x_1-x_3)+\phi^t_P(x_3)\{t(x_1-x_2)\\ &+\ s(x_2-x_3)\}\Big]+\phi^p_B(x_1)\phi^t_\psi(x_2)\phi^t_P(x_3)4m_1m_2m_c\mu_P\Big\}E_n(t_d)\alpha_s(t_d),\end{aligned}\tag{B17}$$

$$\begin{aligned}\mathcal{A}_{d,L}^{LL} &= \frac{1}{N_c}\int_0^1 \mathrm{d}x_1\int_0^1 \mathrm{d}x_2\int_0^1 \mathrm{d}x_3\int_0^\infty \mathrm{d}b_1\int_0^\infty b_2\,\mathrm{d}b_2\int_0^\infty b_3\,\mathrm{d}b_3\,\delta(b_1-b_3)H_n(\alpha,\beta_d,b_2,b_3)\\ &\times\left\{\phi_B^a(x_1)\phi_V^v(x_3)\left[\phi_\psi^v(x_2)s\{u(x_1-x_3)+t(x_1-x_2)\}+\phi_\psi^t(x_2)m_2m_cu\right]\right.\\ &+\phi_B^p(x_1)\phi_\psi^v(x_2)m_1m_3\left[\phi_V^s(x_3)2m_1p(x_3-x_1)+\phi_V^t(x_3)\{t(x_2-x_1)\right.\\ &\left.\left.+s(x_3-x_2)\}\right]-\phi_B^p(x_1)\phi_\psi^t(x_2)\phi_V^t(x_3)m_1m_3(t-s)\frac{2m_c}{m_2}\right\}E_n(t_d)\alpha_s(t_d),\end{aligned}\tag{B18}$$

$$\begin{aligned}\mathcal{A}_{d,N}^{LL} &= \frac{1}{N_c}\int_0^1 \mathrm{d}x_1\int_0^1 \mathrm{d}x_2\int_0^1 \mathrm{d}x_3\int_0^\infty \mathrm{d}b_1\int_0^\infty b_2\,\mathrm{d}b_2\int_0^\infty b_3\,\mathrm{d}b_3\,\delta(b_1-b_3)H_n(\alpha,\beta_d,b_2,b_3)\\ &\times E_n(t_d)\alpha_s(t_d)\left\{\phi_B^a(x_1)m_3\left[\phi_\psi^V(x_2)\phi_V^V(x_3)2m_2\{u(x_1-x_3)+t(x_1-x_2)\}\right.\right.\\ &\left.+\phi_\psi^T(x_2)m_c\{\phi_V^V(x_3)t+\phi_V^A(x_3)2m_1p\}\right]-\phi_B^p(x_1)\phi_\psi^T(x_2)\phi_V^T(x_3)2m_1m_cs\\ &\left.+\phi_B^p(x_1)\phi_\psi^V(x_2)\phi_V^T(x_3)m_1m_2\{u(x_3-x_1)+s(x_2-x_3)\}\right\},\end{aligned}\tag{B19}$$

$$\begin{aligned}\mathcal{A}_{d,T}^{LL} &= \frac{1}{N_c}\int_0^1 \mathrm{d}x_1\int_0^1 \mathrm{d}x_2\int_0^1 \mathrm{d}x_3\int_0^\infty \mathrm{d}b_1\int_0^\infty b_2\,\mathrm{d}b_2\int_0^\infty b_3\,\mathrm{d}b_3\,\delta(b_1-b_3)H_n(\alpha,\beta_d,b_2,b_3)\\ &\times E_n(t_d)\alpha_s(t_d)\left\{\phi_B^a(x_1)\left[\phi_\psi^V(x_2)\phi_V^A(x_3)\frac{2m_2m_3}{m_1p}\{u(x_3-x_1)+t(x_2-x_1)\}\right.\right.\\ &\left.-\phi_\psi^T(x_2)m_3m_c\{2\phi_V^V(x_3)+\phi_V^A(x_3)\frac{t}{m_1p}\}\right]+\phi_B^p(x_1)\phi_\psi^T(x_2)\phi_V^T(x_3)4m_1m_c\\ &\left.+\phi_B^p(x_1)\phi_\psi^V(x_2)\phi_V^T(x_3)2m_1m_2(x_1-x_2)\right\},\end{aligned}\tag{B20}$$

$$\begin{aligned}\mathcal{A}_{d,P}^{LR} &= \frac{1}{N_c}\int_0^1 \mathrm{d}x_1\int_0^1 \mathrm{d}x_2\int_0^1 \mathrm{d}x_3\int_0^\infty \mathrm{d}b_1\int_0^\infty b_2\,\mathrm{d}b_2\int_0^\infty b_3\,\mathrm{d}b_3\,H_n(\alpha,\beta_d,b_2,b_3)\\ &\times E_n(t_d)\left\{\phi_B^a(x_1)\phi_P^a(x_3)2m_1p\left[\phi_\psi^v(x_2)\{u(x_3-x_1)+s(x_2-x_3)\}\right.\right.\\ &\left.+\phi_\psi^t(x_2)m_2m_c\right]+\phi_B^p(x_1)\phi_\psi^v(x_2)m_1\mu_P\left[\phi_P^p(x_3)2m_1p(x_1-x_3)\right.\\ &\left.\left.+\phi_P^t(x_3)\{t(x_2-x_1)+s(x_3-x_2)\}\right]\right\}\alpha_s(t_d)\delta(b_1-b_3),\end{aligned}\tag{B21}$$

$$\begin{aligned}\mathcal{A}_{d,L}^{LR} &= \frac{1}{N_c}\int_0^1 \mathrm{d}x_1\int_0^1 \mathrm{d}x_2\int_0^1 \mathrm{d}x_3\int_0^\infty \mathrm{d}b_1\int_0^\infty b_2\,\mathrm{d}b_2\int_0^\infty b_3\,\mathrm{d}b_3\,H_n(\alpha,\beta_d,b_2,b_3)\\ &\times E_n(t_d)\left\{\phi_B^p(x_1)\phi_\psi^v(x_2)m_1m_3\left[\phi_V^t(x_3)\{s(x_2-x_3)+t(x_1-x_2)\}\right.\right.\\ &\left.+\phi_V^s(x_3)2m_1p(x_3-x_1)\right]-\phi_B^a(x_1)\phi_V^v(x_3)\left[\phi_\psi^t(x_2)m_2m_cu\right.\\ &\left.\left.+\phi_\psi^v(x_2)4m_1^2p^2(x_2-x_1)\right]\right\}\alpha_s(t_d)\delta(b_1-b_3),\end{aligned}\tag{B22}$$

$$\begin{aligned}\mathcal{A}_{d,N}^{LR} &= \frac{1}{N_c}\int_0^1 \mathrm{d}x_1\int_0^1 \mathrm{d}x_2\int_0^1 \mathrm{d}x_3\int_0^\infty \mathrm{d}b_1\int_0^\infty b_2\,\mathrm{d}b_2\int_0^\infty b_3\,\mathrm{d}b_3\,H_n(\alpha,\beta_d,b_2,b_3)\\ &\times E_n(t_d)\left\{\phi_B^p(x_1)\phi_\psi^V(x_2)\phi_V^T(x_3)m_1m_2\{u(x_1-x_3)+s(x_3-x_2)\}\right.\\ &\left.+\phi_B^a(x_1)\phi_\psi^T(x_2)m_3m_c\left[\phi_V^A(x_3)2m_1p-\phi_V^V(x_3)t\right]\right\}\alpha_s(t_d)\delta(b_1-b_3),\end{aligned}\tag{B23}$$

$$\begin{aligned}\mathcal{A}^{LR}_{d,T} &= \frac{1}{N_c}\int_0^1 \mathrm{d}x_1\int_0^1 \mathrm{d}x_2\int_0^1 \mathrm{d}x_3\int_0^\infty \mathrm{d}b_1\int_0^\infty b_2\mathrm{d}b_2\int_0^\infty b_3\mathrm{d}b_3 H_n(\alpha,\beta_d,b_2,b_3)\\ &\times E_n(t_d)\alpha_s(t_d)\Big\{\phi^a_B(x_1)\phi^T_\psi(x_2)m_3m_c\Big[\phi^A_V(x_3)\frac{t}{m_1p}-2\phi^V_V(x_3)\Big]\\ &+ \phi^p_B(x_1)\phi^V_\psi(x_2)\phi^T_V(x_3)2m_1m_2(x_2-x_1)\Big]\Big\}\delta(b_1-b_3),\end{aligned} \tag{B24}$$

where x_i and b_i are the longitudinal momentum fraction and the conjugate variable of the transverse momentum k_{iT}, respectively. The subscript i of $\mathcal{A}^k_{i,j}$ corresponds to the indices of Fig. 2; the subscript $j = P$, L, N, T corresponds to the different helicity amplitudes; and the superscript k refers to the two possible Dirac structures $\Gamma_1\otimes\Gamma_2$ of the operators $(\bar{q}_1q_2)_{\Gamma_1}(\bar{q}_3q_4)_{\Gamma_2}$, namely $k = LL$ for $(V-A)\otimes(V-A)$ and $k = LR$ for $(V-A)\otimes(V+A)$.

The function $H_{f,n}$ and Sudakov factor $E_{f,n}$ are defined as:

$$H_f(\alpha,\beta,b_i,b_j) = K_0(b_i\sqrt{-\alpha})\Big\{\theta(b_i-b_i)K_0(b_i\sqrt{-\beta})I_0(b_j\sqrt{-\beta})+(b_i\leftrightarrow b_j)\Big\}, \tag{B25}$$

$$\begin{aligned}H_n(\alpha,\beta,b_i,b_j) &= \Big\{\theta(-\beta)K_0(b_i\sqrt{-\beta})+\frac{\pi}{2}\theta(\beta)\Big[iJ_0(b_i\sqrt{\beta})-Y_0(b_i\sqrt{\beta})\Big]\Big\}\\ &\times\Big\{\theta(b_i-b_j)K_0(b_j\sqrt{-\alpha})I_0(b_j\sqrt{-\alpha})+(b_i\leftrightarrow b_j)\Big\},\end{aligned} \tag{B26}$$

$$E_f(t) = \exp\{-S_B(t)-S_M(t)\}, \tag{B27}$$

$$E_n(t) = \exp\{-S_B(t)-S_M(t)-S_\psi(t)\}, \tag{B28}$$

$$S_B(t) = s(x_1,b_1,p_1^+)+2\int_{1/b_1}^t\frac{\mathrm{d}\mu}{\mu}\gamma_q, \tag{B29}$$

$$S_M(t) = s(x_3,b_3,p_3^+)+s(\bar{x}_3,b_3,p_3^+)+2\int_{1/b_3}^t\frac{\mathrm{d}\mu}{\mu}\gamma_q, \tag{B30}$$

$$S_\psi(t) = s(x_2,b_2,p_2^+)+s(\bar{x}_2,b_2,p_2^+)+2\int_{1/b_2}^t\frac{\mathrm{d}\mu}{\mu}\gamma_q, \tag{B31}$$

where I_0, J_0, K_0 and Y_0 are Bessel functions; $\gamma_q = -\alpha_s/\pi$ is the quark anomalous dimension; the expression of $s(x,b,Q)$ can be found in the appendix of Ref. [40]; and α and β are the virtualities of gluon and quarks. The subscript of the quark virtuality β_i corresponds to the indices of Fig. 2. The definitions of the particle virtuality and typical scale t_i are given as follows:

$$\alpha = x_1^2m_1^2+x_3^2m_3^2-x_1x_3u, \tag{B32}$$

$$\beta_a = x_3^2m_3^2-x_3u+m_1^2-m_b^2, \tag{B33}$$

$$\beta_b = x_1^2m_1^2-x_1u+m_3^2, \tag{B34}$$

$$\beta_c = \alpha+\bar{x}_2^2m_2^2-x_1\bar{x}_2t+\bar{x}_2x_3s-m_c^2, \tag{B35}$$

$$\beta_d = \alpha+x_2^2m_2^2-x_1x_2t+x_2x_3s-m_c^2, \tag{B36}$$

$$t_i = \max(\sqrt{|\alpha|},\sqrt{|\beta_i|},1/b_1,1/b_2,1/b_3). \tag{B37}$$

References

1 C. Patrignani et al (Particle Data Group), Chin. Phys. C, **40**: 100001 (2016)
2 J. Segovia, D. Entem, F. Fernández, Nucl. Phys. A, **915**: 125 (2013)
3 J. Sun, Y. Yang, N. Wang, Q. Chang, G. Lu, Int. J. Theor. Phys., **56**: 1892 (2017)
4 G. Buchalla, A. Buras, M. Lautenbacher, Rev. Mod. Phys., **68**: 1125, (1996)
5 N. Cabibbo, L. Maiani, Phys. Lett. B, **73**: 418 (1978)
6 D. Fakirov, B. Stech, Nucl. Phys. B, **133**: 315 (1978)
7 M. Bauer, B. Stech, M. Wirbel, Z. Phys. C, **34**: 103 (1987)
8 J. Bjorken, Nucl. Phys. B (Proc. Suppl.), **11**: 325 (1989)
9 J. Li, D. Du, Phys. Rev. D, **78**: 074030 (2008)
10 B. Melić, Phys. Rev. D **68**: 034004 (2003)
11 B. Melić, Phys. Lett. B, **591**: 91 (2004)
12 X. Liu, Z. Zhang, Z. Xiao, Chin. Phys. C, **34**: 937 (2010)
13 X. Liu, W. Wang, Y. Xie, Phys. Rev. D, **89**: 094010 (2014)
14 C. Chen, H. Li, Phys. Rev. D, **71**: 114008 (2005)
15 Z. Rui, Y. Li, Z. Xiao, Eur. Phys. J. C, **77**: 610 (2017)
16 Z. Zhang, Phys. Lett. B, **772**: 719 (2017)
17 H. Cheng, K. Yang, Phys. Rev. D, **63**: 074011 (2001)
18 H. Cheng, Y. Keum, K. Yang, Phys. Rev. D, **65**: 094023 (2002)
19 M. Beneke, G. Buchalla, M. Neubert, C. Sachrajda, Phys. Rev. Lett., **83**: 1914 (1999)
20 M. Beneke, G. Buchalla, M. Neubert, C. Sachrajda, Nucl. Phys. B, **591**: 313 (2000)
21 D. Du, D. Yang, G. Zhu, Phys. Lett. B, **488**: 46 (2000)
22 M. Beneke, G. Buchalla, M. Neubert, C. Sachrajda, Nucl. Phys. B, **606**: 245 (2001)

23 D. Du, D. Yang, G. Zhu, Phys. Lett. B, **509**: 263 (2001)
24 D. Du, D. Yang, G. Zhu, Phys. Rev. D, **64**: 014036 (2001)
25 M. Beneke, J. Rohrer, D. Yang, Nucl. Phys. B, **774**: 64 (2007)
26 J. Sun, G. Xue, Y. Yang, G. Lu, D. Du, Phys. Rev. D, **77**: 074013 (2008)
27 J. Virto, arXiv:1609.07430 and Refs[23-33] therein
28 M. Beneke, M. Neubert, Nucl. Phys. B, **675**: 333 (2003)
29 G. Bell, Nucl. Phys. B, **795**: 1 (2008)
30 G. Bell, Nucl. Phys. B, **822**: 172 (2009)
31 M. Beneke, T. Huber, X. Li, Nucl. Phys. B, **832**: 109 (2010)
32 C. Kim, Y. Yoon, JHEP, **1111**: 003 (2011)
33 M. Beneke, T. Huber, X. Li, Phys. Lett. B, **750**: 348 (2015)
34 M. Beneke, S. Jäger, Nucl. Phys. B, **751**: 160 (2006)
35 M. Beneke, S. Jäger, Nucl. Phys. B, **768**: 51 (2007)
36 N. Kivel, JHEP, **0705**: 019 (2007)
37 V. Pilipp, Nucl. Phys. B, **794**: 154 (2008)
38 H. Li, H. Yu, Phys. Rev. Lett., **74**: 4388 (1995)
39 H. Li, Phys. Lett. B, **348**: 597 (1995)
40 H. Li, Phys. Rev. D, **52**: 3958 (1995)
41 C. Chang, H. Li, Phys. Rev. D, **55**: 5577 (1997)
42 T. Yeh, H. Li, Phys. Rev. D, **56**: 1615 (1997)
43 Y. Keum, H. Li, Phys. Rev. D, **63**: 074006 (2001)
44 Y. Keum, H. Li, A. Sanda, Phys. Lett. B, **504**: 6 (2001)
45 Y. Keum, H. Li, A. Sanda, Phys. Rev. D, **63**: 054008 (2001)
46 C. Lü, K. Ukai, M. Yang, Phys. Rev. D, **63**: 074009 (2001)
47 C. Lü, M. Yang, Eur. Phys. J. C, **23**: 275 (2002)
48 A. Bradley, A. Khare, Z. Phys. C, **8**: 131 (1981)
49 A. Badalian, I. Danilkin, Phys. Atom. Nucl., **72**: 1206 (2009)
50 B. Li, K. Chao, Phys. Rev. D, **79**: 094004 (2009)
51 A. Badalian, B. Bakker, I. Danilkin, Phys. Atom. Nucl., **72**: 638 (2009)
52 K. Chao, Phys. Lett. B, **661**: 348 (2008)
53 M. Anwar, Y. Lu, B. Zou, Phys. Rev. D, **95**: 114031 (2017)
54 A. Badalian, B. Bakker, Phys. Rev. D, **96**: 014030 (2017)
55 Y. Kuang, T. Yan, Phys. Rev. D, **41**: 155 (1990)
56 Y. Ding, D. Qin, K. Chao, Phys. Rev. D, **44**: 3562 (1991)
57 J. Rosner, Phys. Rev. D, **64**: 094002 (2001)
58 K. Liu, K. Chao, Phys. Rev. D, **70**: 094001 (2004)
59 V. Novikov, L. Okun, M. Shifman, A. Vainshtein et al, Phys. Rept., **41**: 1 (1978)
60 J. Richard, Z. Phys. C, **4**: 211 (1980)
61 J. Segovia, D. Entem, F. Fernandez, E. Hernandez, Int. J. Mod. Phys. E, **22**: 1330026 (2013)
62 W. Deng, H. Liu, L. Gui, X. Zhong, Phys. Rev. D, **95**: 034026 (2017) and references therein.
63 D. Molina, M. Sanctis, C. Fernández-Ramírez, Phys. Rev. D, **95**: 094021 (2017)
64 N. Soni, B. Joshi, R. Shah, H. Chauhan, J. Pandya, Eur. Phys. J. C, **78**: 592 (2018)
65 G. Lepage, S. Brodsky, Phys. Rev. D, **22**: 2157 (1980)
66 P. Ball, V. Braun, Y. Koike, K. Tanaka, Nucl. Phys. B, **529**: 323 (1998)
67 T. Kurimoto, H. Li, A. Sanda, Phys. Rev. D, **65**: 014007 (2001)
68 P. Ball, JHEP, **9901**: 010 (1999)
69 P. Ball, G. Jones, JHEP, **0703**: 069 (2007)
70 P. Ball, V. Braun, A. Lenz, JHEP, **0605**: 004 (2006)
71 J. Sun, Q. Li, Y. Yang, H. Li, Q. Chang, Z. Zhang, Phys. Rev. D, **92**: 074028 (2015)
72 Y. Yang, J. Sun, Y. Guo, Q. Li, J. Huang, Q. Chang, Phys. Lett. B, **751**: 171 (2015)
73 J. Sun, Y. Yang, Q. Li, H. Li, Q. Chang, J. Huang, Phys. Lett. B, **752**: 322 (2016)
74 J. Sun, J. Gao, Y. Yang, Q. Chang et al, Phys. Rev. D, **96**: 036010 (2017)
75 G. Lepage, L. Magnea, C. Nakhleh, U. Magnea, K. Hornbostel, Phys. Rev. D, **46**: 4052 (1992)
76 G. Bodwin, E. Braaten, G. Lepage, Phys. Rev. D, **51**: 1125 (1995)
77 N. Brambilla, A. Pineda, J. Soto, A. Vairo, Rev. Mod. Phys., **77**: 1423 (2005)
78 R. Barbieri, R. Gatto, R. Kögerler, Z. Kunszt, Phys. Lett. B, **57**: 455 (1975)
79 R. Barbieri, R. Kögerler, Z. Kunszt, R. Gatto, Nucl. Phys. B, **105**: 125 (1976)
80 W. Celmaster, Phys. Rev. D, **19**: 1517 (1979)
81 E. Poggio, H. Schnitzer, Phys. Rev. D, **20**: 1175 (1979)
82 E. Eichten, K. Gottfried, T. Kinoshita, K. Lane, T. Yan, Phys. Rev. D, **21**: 203 (1980)
83 A. Bradley, F. Gault, Z. Phys. C, **5**: 239 (1980)
84 J. Erler, Phys. Rev. D, **59**: 054008 (1999)
85 C. Chen, Y. Keum, H. Li, Phys. Rev. D, **66**: 054013 (2002)
86 Y. Yang, J. Sun, J. Gao, Q. Chang, J. Huang, G. Lu, Int. J. Mod. Phys. A, **31**: 1650146 (2016)
87 J. Sun, Y. Yang, J. Huang, G. Lu, Q. Chang, Nucl. Phys. B, **911**: 890 (2016)
88 J. Sun, Y. Yang, N. Wang, J. Huang, Q. Chang, Phys. Rev. D, **95**: 036024 (2017)
89 B. Xiao, X. Qin, B. Ma, Eur. Phys. J. A, **15**: 523 (2002)